Mycologia, 103(6), 2011, pp. 1384–1410. DOI: 10.3852/11-006

Novel species of *Celoporthe* from *Eucalyptus* and *Syzygium* trees in China and Indonesia

ShuaiFei Chen

Department of Microbiology and Plant Pathology, Forestry and Agricultural Biotechnology Institute (FABI), University of Pretoria, Pretoria 0002, South Africa, and China Eucalypt Research Centre (CERC), Chinese Academy of Forestry (CAF), ZhanJiang, 524022, GuangDong Province, China

Marieka Gryzenhout
Jolanda Roux

Department of Microbiology and Plant Pathology, Forestry and Agricultural Biotechnology Institute (FABI), University of Pretoria, Pretoria 0002, South Africa

YaoJian Xie

China Eucalypt Research Centre (CERC), Chinese Academy of Forestry (CAF), ZhanJiang 524022, GuangDong Province, China

Michael J. Wingfield

Department of Microbiology and Plant Pathology, Forestry and Agricultural Biotechnology Institute (FABI), University of Pretoria, Pretoria 0002, South Africa

XuDong Zhou[1]

Department of Microbiology and Plant Pathology, Forestry and Agricultural Biotechnology Institute (FABI), University of Pretoria, Pretoria 0002, South Africa, and China Eucalypt Research Centre (CERC), Chinese Academy of Forestry (CAF), ZhanJiang 524022, GuangDong Province, China

Abstract: Many species in the Cryphonectriaceae cause diseases of trees, including those in the genera *Eucalyptus* and *Syzygium*. During disease surveys on these trees in southern China, fruiting structures typical of fungi in the Cryphonectriaceae and associated with dying branches and stems were observed. Morphological comparisons suggested that these fungi were distinct from the well known *Chrysoporthe deuterocubensis*, also found on these trees in China. The aim of this study was to identify these fungi and evaluate their pathogenicity to *Eucalyptus* clones/species as well as *Syzygium cumini*. Three morphologically similar fungal isolates collected previously from Indonesia also were included in the study. Isolates were characterized based on comparisons of morphology and DNA sequence data for the partial LSU and ITS nuclear ribosomal DNA, β-tubulin and *TEF-1*α gene regions. After glasshouse trials to select virulent isolates field inoculations were undertaken to screen different commercial *Eucalyptus* clones/species and *S. cumini* trees for susceptibility to infection. Phylogenetic analyses showed that the Chinese isolates and those from Indonesia reside in a clade close to previously identified South African *Celoporthe* isolates. Based on morphology and DNA sequence comparisons, four new *Celoporthe* spp. were identified and they are described as *C. syzygii*, *C. eucalypti*, *C. guangdongensis* and *C. indonesiensis*. Field inoculations indicated that the three Chinese *Celoporthe* spp., *C. syzygii*, *C. eucalypti* and *C. guangdongensis*, are pathogenic to all tested *Eucalyptus* and *S. cumini* trees. Significant differences in the susceptibility of the inoculated *Eucalyptus* clones/species suggest that it will be possible to select disease-tolerant planting stock for forestry operations in the future.

Key words: Cryphonectriaceae, Myrtales, plantation forestry, southeastern Asia, stem canker pathogens

INTRODUCTION

The Cryphonectriaceae Gryzenh. & M.J. Wingf. (Diaporthales) represents a group of bark and/or wood-infecting fungi of trees and shrubs in various parts of the world (Gryzenhout et al. 2009). Species of Cryphonectriaceae exist naturally as virulent pathogens, facultative parasites or saprophytes on woody hosts. Some species have been introduced into new environments, causing diseases on important trees, such as those grown commercially in plantations or for their ornamental value, and include some of the most important tree pathogens in the world (Gryzenhout et al. 2009). Except for *Cryphonectria* (Sacc.) Sacc. & D. Sacc., which is the type genus, 13 other genera have been described in this family (Nakabonge et al. 2006a; Cheewangkoon et al. 2009; Gryzenhout et al. 2009, 2010; Begoude et al. 2010; Vermeulen et al. 2011).

Several species of Cryphonectriaceae had been collected from trees in China. *Cryphonectria parasitica* (Murrill) M.E. Barr, best known for causing a devastating canker disease of chestnuts (*Castanea* spp.) in USA and Europe (Anagnostakis 1987, 1992), also causes cankers and dieback on Chinese chestnut (*Castanea mollissima* Blume) trees in their native range (Fairchild 1913; Shear and Stevens 1913, 1916).

Submitted 5 Jan 2011; accepted for publication 19 Apr 2011.
[1] Corresponding author. E-mail: xu.zhou@fabi.up.ac.za OR cerc.zhou@gmail.com

Cryphonectria japonica (Tak. Kobay. & Kaz. Itô) Gryzenh. & M.J. Wingf. (= *Cryphonectria nitschkei* [G.H. Otth] M.E. Barr), which first was collected in Japan, and *Endothia gyrosa* (Schwein.: Fr.) Fr. have been found on a *Quercus* sp. in China (Teng 1934, Kobayashi and Itô 1956, Myburg et al. 2004, Gryzenhout et al. 2009). *Chrysoporthe deuterocubensis* Gryzenh. & M.J. Wingf., treated as *Chr. cubensis* (Bruner) Gryzenh. & M.J. Wingf. (van der Merwe et al. 2010), has been reported from species of *Eucalyptus* and *Syzygium* in southern China from a wide range of locations (Sharma et al. 1985, Hodges et al. 1986, Myburg et al. 2002, Zhou et al. 2008, Chen et al. 2010).

The genus *Celoporthe* Nakab., Gryzenh., Jol. Roux & M.J. Wingf., based on *C. dispersa* Nakab., Gryzenh., Jol. Roux & M.J. Wingf., is a recently described genus in the Cryphonectriaceae, reported from dying branches and stems on both native and introduced Myrtales in South Africa (Nakabonge et al. 2006a). *Celoporthe* is monotypic, but phylogenetic analyses have shown that it is composed of three distinct phylogenetic clades (Nakabonge et al. 2006a). *C. dispersa* is represented by isolates from native *Syzygium cordatum* Hochst.: C.Kraus, native *Heteropyxis canescens* Oliv. and non-native *Tibouchina granulosa* Cogn. (Nakabonge et al. 2006a) in South Africa. Based on DNA sequence comparisons, isolates collected from *Syzygium aromaticum* (L.) Merr. & L.M. Perry in Indonesia (Myburg et al. 2003) also grouped closely with *C. dispersa*, but morphological evaluation was impossible because relative herbarium material does not exist (Myburg et al. 2003).

During surveys in southern China for pathogens of trees in the Myrtaceae, especially species of *Eucalyptus* and *Syzygium*, several species affecting these trees were identified (Zhou et al. 2008). In addition to *Chr. deuterocubensis* (Chen et al. 2010) these surveys yielded a fungus on *Eucalyptus* and *S. cumini* trees resembling *C. dispersa*. The aim of the present study was to characterize these isolates based on morphology and phylogenetic analyses and to assess their pathogenicity to *Eucalyptus* and *S. cumini* with glasshouse and field inoculations.

MATERIALS AND METHODS

Sampling.—*Eucalyptus* (Myrtales) plantations in the Guang-Dong Province of southern China were investigated for the presence of fungal diseases Nov–Dec 2006, Jan 2007 and Sep–Nov 2008. Where present in these areas *S. cumini* trees (Myrtales) also were examined for the presence of fungi in the Cryphonectriaceae because these fungi are known to occur on *Syzygium* spp. (Heath et al. 2006, Gryzenhout et al. 2009). Sections of bark bearing fruiting structures (ascostromata and conidiomata) resembling the Cryphonectriaceae were collected from symptomatic trees and transported to the laboratory to make isolations.

Samples were incubated in moist chambers 1–3 d to induce the production of spores from the fruiting bodies. Single tendrils of spores were transferred to 2% malt extract agar (MEA) (Biolab, Merck, Midrand, South Africa) (20 g Biolab malt extract, 20 g Biolab agar, 1 L water) and incubated at 25 C. Single hyphal tips were transferred to fresh 2% MEA to obtain pure cultures. Three unidentified isolates from Indonesia, originating from *S. aromaticum* and resembling fungi in the Cryphonectriaceae, obtained from the culture collection (CMW) of the Forestry and Agricultural Biotechnology Institute (FABI), University of Pretoria, South Africa, also were included in this study (TABLE I). All cultures collected from China are maintained in the culture collection (CMW), and a duplicate set of isolates is maintained in a culture collection at the China Eucalypt Research Centre (CERC), Chinese Academy of Forestry (CAF), China. Representative isolates also were deposited with the Centraalbureau voor Schimmelcultures (CBS), Utrecht, the Netherlands (TABLE I). The original bark bearing fruiting structures was deposited in the National Collection of Fungi (PREM), Pretoria, South Africa.

DNA extraction, PCR and sequencing reactions.—Isolates originating from different *Eucalyptus* species/clones and *S. cumini* from the various areas sampled, as well as those showing differing culture and fruiting structure morphology (TABLE I), were selected for DNA sequence comparisons. Before DNA extraction, isolates were grown in 2% MEA at 25 C for 5–7 d. For each isolate actively growing mycelium from one MEA plate per isolate was scraped from the surface of the medium with a sterile scalpel and transferred to 1.5 mL Eppendorf tubes. Genomic DNA was extracted with the method described by Myburg et al. (1999), separated by electrophoresis on a 1% agarose gel, stained with ethidium bromide and viewed under ultraviolet (UV) light. Samples were treated with 3 µL RNase (1 mg/mL) and left overnight at 37 C to degrade RNA.

Gene regions amplified with the polymerase chain reaction (PCR) included the conserved nuclear large subunit (LSU) ribosomal DNA, the β-tubulin gene region 1 (*BT1*) and 2 (*BT2*), the internal transcribed spacer (ITS) regions including the 5.8S gene of the ribosomal DNA operon as well as the translation elongation factor 1-alpha (*TEF-1α*) gene region. Part of the LSU rDNA gene region was amplified with primers LR0R and LR7 (Vilgalys and Hester 1990, Rehner and Samuels 1994); two regions within the *BT* gene were amplified respectively with primer pairs βt1a/βt1b and βt2a/βt2b (Glass and Donaldson 1995); the ITS regions including the 5.8S rDNA operon were amplified with the primer pair ITS1 and ITS4 (White et al. 1990); and a fragment of the *TEF-1α* gene region was amplified with primer pairs EF1-728F and EF1-986R (Carbone and Kohn 1999). PCR conditions for the LSU gene region were as outlined by Castlebury et al. (2002); those for the *BT1/2* and ITS gene regions followed the protocols of Myburg et al. (2002); and the *TEF-1α* gene region was amplified with the method described by Slippers et al. (2004). PCR products were viewed with UV light on 1% agarose

TABLE I. Isolates generated and used for phylogenetic analyses and pathogenicity trials in this study

Species	Culture number[a]	Other number	Host	Location	Collector[b]	GenBank accession number[c]				
						BT1	*BT2*	ITS	*TEF-1α*	LSU
Aurifilum marmelostoma	CMW28285	CBS124929	*Terminalia mantaly*	Yaounde, Cameroon	DB & JR	FJ900585	FJ900590	FJ882855	n/a[d]	**HQ730873**
	CMW28288	CBS124930	*T. ivorensis*	Mbalmayo,Cameroon	DB & JR	FJ900586	FJ900591	FJ882856	n/a	**HQ730874**
Celoporthe dispersa	CMW9976	CBS118782	*Syzygium cordatum*	Limpopo, South Africa	MG	DQ267136	DQ267142	DQ267130	HQ730840	**HQ730853**
	CMW9978	CBS118781	*S. cordatum*	Limpopo, South Africa	MG	DQ267135	DQ267141	AY214316	HQ730841	**HQ730854**
C. eucalypti	CMW26900[e]	CBS127191	*Eucalyptus* EC48 clone	GuangDong, China	XDZ & SFC	**HQ730816**	**HQ730826**	**HQ730836**	**HQ730849**	**HQ730862**
	CMW26908[efg]	CBS127190	*Eucalyptus* EC48 clone	GuangDong, China	XDZ & SFC	**HQ730817**	**HQ730827**	**HQ730837**	**HQ730850**	**HQ730863**
	CMW26911[e]	CBS127192	*Eucalyptus* EC48 clone	GuangDong, China	XDZ & SFC	**HQ730818**	**HQ730828**	**HQ730838**	**HQ730851**	**HQ730864**
	CMW26913		*Eucalyptus* EC48 clone	GuangDong, China	XDZ & SFC	**HQ730819**	**HQ730829**	**HQ730839**	**HQ730852**	**HQ730865**
C. guangdongensis	CMW12750[fg]	CBS128341	*Eucalyptus* sp.	GuangDong, China	TIB	**HQ730810**	**HQ730820**	**HQ730830**	**HQ730843**	**HQ730856**
C. indonesiensis	CMW10781	CBS115844	*S. aromaticum*	North Sumatra, Indonesia	MJW	AY084021	AY084033	AY084009	**HQ730842**	**HQ730855**
	CMW10779		*S. aromaticum*	Somosir, Indonesia	MJW	AY084019	AY084031	AY084007	n/a	n/a
	CMW10780		*S. aromaticum*	Somosir, Indonesia	MJW	AY084020	AY084032	AY084008	n/a	n/a
Celoporthe sp.	CMW14853	CBS534.82	*S. aromaticum*	Indonesia	SM	n/a	n/a	n/a	n/a	AF277142
C. syzygii	CMW34023	CBS127218	*S. cumini*	GuangDong, China	SFC	**HQ730811**	**HQ730821**	**HQ730831**	**HQ730844**	**HQ730857**
	CMW34024		*S. cumini*	GuangDong, China	SFC	**HQ730812**	**HQ730822**	**HQ730832**	**HQ730845**	**HQ730858**
	CMW24912[fg]	CBS127188	*S. cumini*	GuangDong, China	MJW & XDZ	**HQ730813**	**HQ730823**	**HQ730833**	**HQ730846**	**HQ730859**
	CMW24914[fg]	CBS127189	*S. cumini*	GuangDong, China	MJW & XDZ	**HQ730814**	**HQ730824**	**HQ730834**	**HQ730847**	**HQ730860**
	CMW24917[fg]		*S. cumini*	GuangDong, China	MJW & XDZ	**HQ730815**	**HQ730825**	**HQ730835**	**HQ730848**	**HQ730861**
Cryptometrion aestuescens	CMW18790	CBS124008	*Eucalyptus grandis*	Sumatra, Indonesia	MJW	GQ369455	GQ369455	GQ369458	n/a	**HQ730869**
	CMW18793	CBS124007	*E. grandis*	Sumatra, Indonesia	MJW	GQ369456	GQ369456	GQ369459	n/a	**HQ730870**
Latruncella aurorae	CMW28274	CBS124904	*Galpinia transvaalica*	Mpumalanga, South Africa	JR	GU726958	GU726958	GU726946	n/a	**HQ730871**
	CMW28276	CBS125526	*G. transvaalica*	Mpumalanga, South Africa	JR	GU726959	GU726959	GU726947	n/a	**HQ730872**

[a] CMW = Culture collection of the Forestry and Agricultural Biotechnology Institute (FABI), University of Pretoria, Pretoria, South Africa; CBS = the Centraalbureau voor Schimmelcultures, Utrecht, The Netherlands.

[b] DB = D. Begoude, JR = J. Roux, MG = M. Gryzenhout, XDZ = X.D. Zhou, SFC = S.F. Chen, TIB = T.I. Burgess, MJW = M.J. Wingfield, SM = S. Mandang.

[c] GenBank numbers in boldface were sequenced in this study.

[d] n/a, not available.

[e] Isolates used for glasshouse pathogenicity tests on an *Eucalyptus grandis* clone.

[f] Isolates used for pathogenicity tests on *Eucalyptus* in field inoculations in China.

[g] Isolates used for pathogenicity tests on *S. cumini* branches in field inoculations in China.

(ethidium bromide-stained) gels. Amplified products were purified as suggested by the manufacturers with 6% Sephadex G-50 columns (Steinheim, Germany).

Each PCR product was sequenced in both directions with the same primers used for PCR reactions. The ABI PRISM™ Big Dye Terminator Cycle Sequencing Ready Reaction Kit 3.1 (Applied Biosystems, Foster City, California) was used to perform the sequencing reactions. Sephadex G-50 columns (6%) were used to purify the sequence products, whereafter electropherograms were generated on an ABI PRISM 3100 autosequencer (Perkin-Elmer Applied Biosystems, Foster City, California). Nucleotide sequences were edited with MEGA4 (Tamura et al. 2007). All sequences obtained in this study were deposited in GenBank (TABLE I).

Phylogenetic analyses.—To determine the generic placement of the isolates collected from *Eucalyptus* and *S. cumini* in southern China, as well as those previously collected in Indonesia, sequences of the LSU gene region were analyzed. These were supplemented by analyses of the conserved 5.8S rDNA and the exon regions of the *BT* (including partial exon 4, exon 5, partial exon 6 and partial exon 7) gene regions for previously described species in the Cryphonectriaceae (Gryzenhout et al. 2009, Begoude et al. 2010, Gryzenhout et al. 2010, Vermeulen et al. 2011). The datasets of Gryzenhout et al. (2006a, 2009) were used as templates for analyses of the LSU. *Togninia minima* (Tul. & C. Tul.) Berl., *T. fraxinopennsylvanica* (T.E. Hinds) Georg Hausner, Eyjólfsd. & J. Reid and *Phaeoacremonium aleophilum* W. Gams, Crous, M.J. Wingf. & Mugnai were used as outgroups (Gryzenhout et al. 2009). Two isolates of *Diaporthe ambigua* Nitschke were used as outgroups for analyses of the 5.8S gene and *BT* exon regions (Gryzenhout et al. 2009). The partition homogeneity test (PHT) as implemented in PAUP* 4.0b10 (Swofford 2002) was used to determine whether conflict existed between the datasets for these two gene regions (Farris et al. 1995, Huelsenbeck et al. 1996) before performing combined analyses in PAUP*.

To determine the species identities and phylogenetic relationships among the isolates from China and previously described species of Cryphonectriaceae sequences of the *BT1, BT2*, ITS and *TEF-1α* gene regions were analyzed separately and in combination. The partition homogeneity test (PHT) in PAUP 4.0b10 also was used to determine whether conflict existed among the three datasets.

All sequences were aligned with the iterative refinement method (FFT-NS-i settings) of the online version of MAFFT 5.667 (Katoh et al. 2002) and edited manually where necessary in MEGA4 (Tamura et al. 2007). The sequence alignments for each of the datasets were deposited in TreeBASE (http://www.treeBASE.org). Three different phylogenetic analyses were conducted for each of the datasets. Maximum parsimony (MP) analyses were performed with PAUP* 4.0b10, maximum likelihood (ML) tests were conducted with PhyML 3.0 (Guindon and Gascuel 2003), and Bayesian analysis with the Markov chain Monte Carlo (MCMC) algorithm were performed as implemented in MrBayes 3.1.2 (Ronquist and Huelsenbeck 2003).

For MP analyses gaps were treated as a fifth character and the characters were unordered and of equal weight with 1000 random addition replicates. The most parsimonious trees were obtained with the heuristic search function and tree bisection and reconstruction (TBR) as branch swapping algorithms. MAXTREES were unlimited and branch lengths of zero were collapsed. A bootstrap analysis (50% majority rule, 1000 replicates) was done to determine the confidence levels of the tree-branching points (Felsenstein 1985). Tree length (TL), consistency index (CI), retention index (RI) and the homoplasy index (HI) were used to assess the trees (Hillis and Huelsenbeck 1992). For ML and Bayesian analyses of each dataset the best models of nucleotide substitution were established respectively with Modeltest 3.7 (Posada and Crandall 1998) and MrModeltest 2.3 (Nylander 2004). For the ML analyses additional ML parameters in PhyML included the retention of the maximum number of 1000 trees and the determination of nodal support by non-parametric bootstrapping with 1000 replicates. For Bayesian analyses four chains were run simultaneously for the MCMC analyses over 1 000 000 generations. After every 100th generation trees were saved. The burn-in number was established graphically from likelihood scores, and the posterior probabilities (50% majority rule) were determined from the remaining trees. MEGA4 was used to construct consensus trees (Tamura et al. 2007).

Morphology.—Only herbarium samples from *S. cumini* were available for detailed study, and collections from *Eucalyptus* species/clones were available only as cultures. Asexual structures of the Cryphonectriaceae are not always produced, and sexual states are almost never induced in culture. For these reasons thin branches of *E. grandis* and *S. cordatum*, a native species of Myrtaceae in South Africa, were used to induce the production of fruiting structures. Freshly cut branch sections (1–2 cm diam × 15 cm long) of *E. grandis* and *S. cordatum* were inoculated artificially under glasshouse conditions with nine single-conidial isolates (CWM10781, CWM12750, CWM24912, CWM24914, CWM24917, CWM26900, CWM26908, CWM26911, CWM26913) that originated from different hosts and locations in China and Indonesia (TABLE I).

Before inoculation branch sections were surface disinfested by swabbing with 75% alcohol. Each section was inoculated by removing a 7 mm diam cambial disk with a cork borer and placing a disk of equivalent size from a 7 d old MEA culture of these fungi into the wound. Sterile MEA disks were placed in wounds, and these served as controls. Each inoculated wound was covered with parafilm (Pechiney Plastic Packing, Chicago, Illinois). In one method the top ends of the sections were coated with melted paraffin and the other ends were placed in containers of water to ensure that the sections continued to absorb water. In a second method both ends of the branch sections were coated with melted paraffin and the inoculated sections were placed in covered plastic boxes on damp paper towels. Three replicates of each treatment were made, including six branches each of an *E. grandis* clone and *S. cordatum* inoculated with each isolate. All inoculated branch sections were incubated at 25 C. After 6 mo incubation fruiting structures formed on the bark were examined.

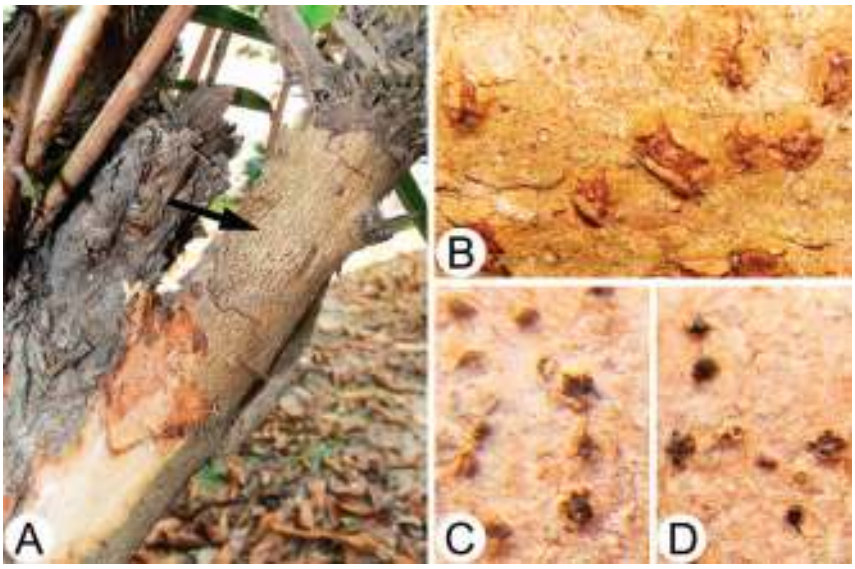

FIG. 1. Symptoms of infection on *S. cumini* trees caused by *C. syzygii*, as well as inoculated branches of *S. cordatum* and an *E. grandis* clone with isolates of a *C. syzygii*. A. Cracks and cankers on *S. cumini* trees caused by *C. syzygii* (arrow indicates fruiting structures). B. Fruiting structures of *C. syzygii* on bark of *S. cumini*. C. Conidiomata of *C. syzygii* on inoculated branches of *S. cordatum*. D. Conidiomata of *C. syzygii* on inoculated branches of an *E. grandis* clone.

To obtain an indication of the minimum and maximum size ranges of the stromata measurements were made from both anamorph and telemorph structures on *Eucalyptus* and *S. cumini* bark. To study the internal morphology of the fungi collected fruiting structures were cut from the original field collected, as well as glasshouse-generated bark specimens under a dissection microscope, boiled 2 min and sectioned (12 µm thick) with a Leica CM1100 cryostat (Setpoint Technologies, Johannesburg, South Africa) at −20 C (Gryzenhout et al. 2004). To study the asci, ascospores, conidiophores, conidiogenous cells and conidia fruiting structures were crushed on microscope slides in 85% lactic acid or 3% KOH. For the holotype specimen 50 measurements were made for each of these characteristics, while 20 measurements per character were made for the remaining specimens. A HRc Axiocam digital camera with Axiovision 3.1 software (Carl Zeiss Ltd., Germany) was used to capture images and to obtain measurements. Characteristics of specimens were compared with those published for closely related species in the Cryphonectriaceae (Gryzenhout et al. 2009, Begoude et al. 2010, Gryzenhout et al. 2010, Vermeulen et al. 2011). The results were presented as (min–) (mean − st.dev.)–(mean + st.dev.) (–max).

For studies of culture characteristics five representative isolates (CMW34023, CMW34024, CMW24912, CMW24914, CMW24917) from *S. cumini*, four isolates (CMW26900, CMW26908, CMW26911, CMW26913) from an *Eucalyptus* clone, one isolate (CMW12750) from an *Eucalyptus* sp., as well as an isolate (CMW10781) from *S. aromaticum* in Indonesia, were used. Isolates were incubated on 2% MEA at 25 C for 7 d. Mycelial plugs (6 mm) were taken from the actively growing margins of these cultures and transferred to the centers of 90 mm Petri dishes containing 2% MEA. These were incubated at 5–35 C at 5 degree intervals with four replicates of each isolate at every temperature. Two measurements perpendicular to each other were taken daily until the fastest growing culture had covered the plate. Averages were computed for each temperature with Microsoft Excel 2003. The entire experiment was repeated once. Color designations were obtained for the descriptions of cultures and fruiting bodies with the charts of Rayner (1970).

Pathogenicity tests.—Glasshouse trials. Three isolates (CMW26900, CMW26908, CMW26911) from an *Eucalyptus* clone in China (TABLE I) were selected for inoculations. These isolates represented a subset of a larger collection of one of the clades identified by DNA sequence comparisons. To select the most virulent isolates for field inoculations in China the three isolates were inoculated on trees of a susceptible *E. grandis* clone (TAG-5) in the glasshouse. The trees were approximately 2 m tall by ~ 10 mm diam. Before conducting inoculations all the trees were allowed to adapt to the glasshouse environment of 25 C with 14 h daylight and 10 h darkness approximately 1 mo. Before inoculation the three isolates were grown at 25 C under continuous fluorescent light 6 d.

Wounds were made on tree bark at the same height (~ 300 mm above the medium) with a cork borer (7 mm diam) to expose the cambium. Agar disks, 7 mm diam, were taken from the margins of actively growing fungal cultures and placed into the wounds with the mycelium facing the exposed cambium. To prevent contamination and desiccation wounds were covered with parafilm. Each of the three isolates was inoculated into the stems of 10 trees. For the negative controls 10 trees were inoculated with sterile MEA plugs. The 40 inoculated trees were arranged randomly in a single glasshouse.

After 6 wk, lesion lengths in the cambium were measured. Small pieces of discolored xylem were taken from four

TABLE II. Statistics resulting from phylogenetic analyses

Dataset	No. of taxa	No. of bp[a]	Maximum parsimony					
			PIC[b]	Number trees	Tree length	CI[c]	RI[d]	HI[e]
LSU	66	639	125	100	283	0.541	0.820	0.459
5.8S rRNA/*BT1/2*	61	760	114 (*5.8S*: 6; *BT*: 108)	1	246	0.581	0.870	0.419
BT1/2	15	874	49	4	69	0.884	0.925	0.116
ITS	15	535	52	1	57	0.947	0.967	0.053
TEF-1α	13	297	27	1	32	0.906	0.933	0.094

Dataset	Maximum likelihood						
	Subst[f] model	NST[g]	Rate matrix	Ti/tv[h] ratio	Rates	I[i]	G[j]
LSU	GTR + I + G	6	(1.4570, 6.3657, 3.7129, 1.3405, 20.3689, 1.0000)		gamma	0.5297	0.511
5.8S rRNA/*BT1/2*	GTR + I	6	(0.3846, 1.9433, 0.2760, 1.0209, 6.3795, 1.0000)		equal	0.7623	
BT1/2	HKY + I	2		1.6439	equal	0.8686	
ITS	TrNef	6	(1.0000, 1.2798, 1.0000, 1.0000, 3.5337, 1.0000)		equal	0	
TEF-1α	HKY	2		2.8872	equal	0	

Dataset	MrBayes				
	Subst[f] model	Prset statefreqpr	NST[g]	Rates	Burn-in
LSU	GTR + I + G	Dirichlet(1,1,1,1)	6	invgamma	100 000
5.8S rRNA/*BT1/2*	GTR + I	Dirichlet(1,1,1,1)	6	propinv	100 000
BT1/2	HKY + I	Dirichlet(1,1,1,1)	2	propinv	50 000
ITS	K80	fixed(equal)	2	equal	100 000
TEF-1α	HKY	Dirichlet(1,1,1,1)	2	equal	50 000

[a] bp = base pairs. [b] PIC = number of parsimony informative characters. [c] CI = consistency index. [d] RI = retention index. [e] HI = homoplasy index. [f] Subst. model = best fit substitution model. [g] NST = number of substitution rate categories. [h] Ti/Tv ratio = transition/transversion ratio. [i] I = proportion of invariable sites. [j] G = gamma distribution shape parameter.

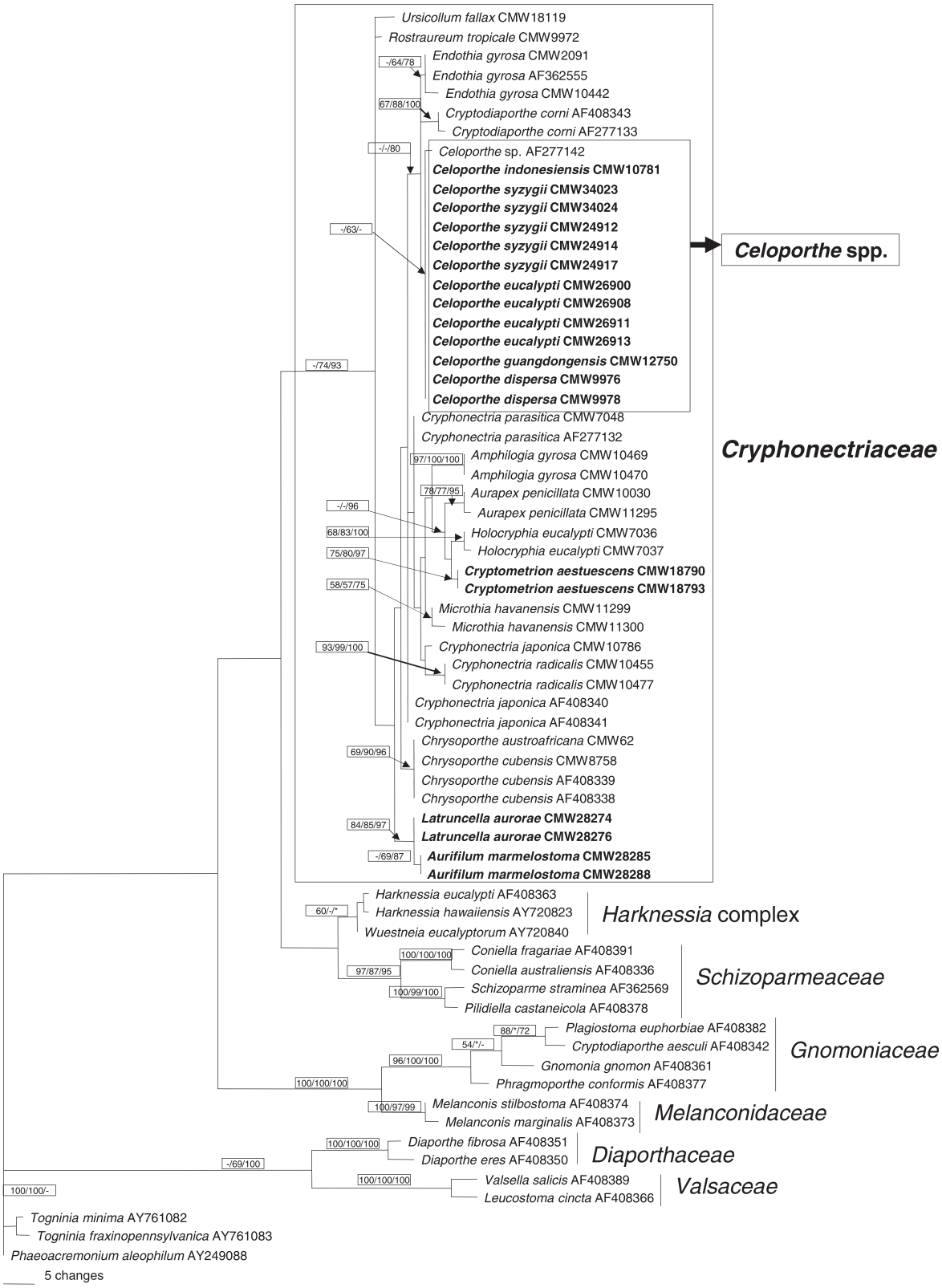

FIG. 2. Cladogram based on maximum parsimony (MP) analysis of *LSU* DNA sequences for various genera in the Diaporthales. Isolates in boldface were sequenced in this study. Sequences with AF and AY numbers originated from Zhang and Blackwell (2001) and Castlebury et al. (2002), while others were obtained from Gryzenhout et al. (2006a, 2009). Bootstrap values > 50% for MP and maximum likelihood (ML), and posterior probabilities > 70% obtained from Bayesian analyses are

randomly selected trees for each isolate as well as all the trees inoculated as controls, placed onto the surface of 2% MEA and incubated at 25 C. In this way it was possible to ascertain that the inoculated fungi were responsible for causing the lesions.

The results of the inoculations were analyzed in SAS 8 with PROC GLM (general linear model) (SAS Institute 1999). To determine the effects of the fungal strains on lesion length, analysis of variance (ANOVA) was conducted. Before ANOVA homogeneity of variance across treatments was confirmed. Fisher's protected test was used to determine the significance among means and $P < 0.05$ for the F value taken as significant in difference.

Field trials. For the field inoculations isolate CMW26908, selected based on the results of the greenhouse trial and isolate CMW12750 also from *Eucalyptus*, were used to test the susceptibility of commercially grown *Eucalyptus* species and clones in southern China (TABLE I). In addition, to compare the aggressiveness of isolates collected from *S. cumini* with the isolates from *Eucalyptus* trees three isolates (CMW24912, CMW24914, CMW24917) collected from *S. cumini* in China (TABLE I) were used. The five isolates selected for field inoculations thus represented three different phylogenetic clades emerging from the DNA sequence comparisons.

Seven *Eucalyptus* genotypes, including hybrids and pure species, were selected for field-inoculation trials. The genotypes included an *E. grandis* clone (CEPT-1), an *E. grandis* × *E. tereticornis* Sm. clone (CEPT-2), an *E. pellita* F.Muell genotype (CEPT-3), two *E. urophylla* S.T.Blake × *E. grandis* clones (CEPT-4, CEPT-7), an *E. urophylla* clone (CEPT-5) and an *E. wetarensis* L.D.Pryor clone (CEPT-6). Isolates CMW12750 and CMW26908 were inoculated on all seven *Eucalyptus* genotypes. Because there were a limited number of *Eucalyptus* trees available for inoculation the isolates (CMW24912, CMW24914, CMW24917) collected from *S. cumini* trees were inoculated only onto *Eucalyptus* genotypes CEPT-6 and CEPT-7.

Inoculated trees were approximately 1 y old at the time of the experiment. For each isolate 6–10 trees of each genotype were inoculated. For the negative controls 10 trees were inoculated with sterile MEA disks. Inoculations were made with a 9 mm diam cork borer to remove the bark and expose the cambium at the same height (~ 400–800 mm) above the ground. Agar disks taken from the actively growing margins of the test isolates were placed in the wounds with the mycelium facing the cambium. In the case of the negative controls, sterile MEA was used. All inoculation wounds were covered with masking tape to reduce contamination and desiccation of the inoculum.

To test the susceptibility of *S. cumini* trees to the fungi isolated from southern China, and also to compare the aggressiveness of isolates collected from *Syzygium* trees with those from *Eucalyptus* on *S. cumini*, the same isolates (CMW12750, CMW26908, CMW24912, CMW24914, CMW24917) as those used for the *Eucalyptus* field tests also were inoculated onto branches of healthy *S. cumini* trees (TABLE I). Ten branches were inoculated for each of the five selected isolates, and 10 *S. cumini* branches were inoculated with sterile MEA as negative controls. Inoculations were conducted with a method similar to that for the *Eucalyptus* genotype inoculation trials. The entire trial was repeated once.

The field trials were conducted Sep–Oct 2008 in ZhanJiang, GuangDong Province, China. After 5 and 6 wk of inoculations on *Eucalyptus* trees and the *S. cumini* branches respectively lesion lengths in the cambium of the trees were measured. Data for lesion length were analyzed with PROC GLM (general linear model) in SAS (SAS Institute 1999) in a manner similar to that for the greenhouse inoculations.

RESULTS

Sampling.—Disease surveys on *Eucalyptus* and *S. cumini* trees in GuangDong Province revealed typical symptoms of infection by fungi in the Cryphonectriaceae. These included cracking of the bark and the formation of girdling stem cankers (FIG. 1A, B). Apart from symptoms caused by *Chr. deuterocubensis* (Chen et al. 2010), anamorph and teleomorph fruiting structures of a fungus resembling *C. dispersa* were observed on diseased bark of *Eucalyptus* and *S. cumini* trees. These fruiting structures (anamorph and teleomorph) often were completely orange with orange to umber perithecial necks, and they could be distinguished from fruiting structures of *Chr. deuterocubensis* that were always fuscous black to umber, with black and much longer perithecial necks (Gryzenhout et al. 2009, Chen et al. 2010). Ascostromata and conidiomata of the unknown fungus often were found on the cankers on the *S. cumini* trees, while only conidiomata were observed on *Eucalyptus* trees. Isolates were obtained from two *S. cumini* trees, one tree of an unknown *Eucalyptus* sp. and one tree representing *Eucalyptus* clone EC48 (TABLE I).

Phylogenetic analyses.—*Generic placement.* The aligned sequences of the LSU dataset consisted of 66 taxa and 639 characters (TreeBASE: http://purl.org/phylo/treebase/phylows/study/TB2:S11111). Statistical values for obtained trees for the parsimony analysis, number of informative characters and parameters for the best

←

presented above branches as follows: MP/ML/Bayesian. Bootstrap values lower than 50%, and posterior probabilities lower than 70% are marked with *, and absent analysis values are marked with −. *Togninia minima* (AY761082), *T. fraxinopennsylvanica* (AY761083) and *Phaeoacremonium aleophilum* (AY249088) in the family Togniniaceae represent the outgroups.

fit substitution models are provided (TABLE II). For maximum parsimony (MP), maximum likelihood (ML) and Bayesian analyses the position of the genera in relation to each other was different, but genera still could be distinguished consistently from each other. A total of 100 most parsimonious trees were obtained after analyses of the LSU dataset, of which the first tree was saved (FIG. 2). Isolates collected from *Eucalyptus* and *S. cumini* trees in China and *S. aromaticum* in Indonesia clearly resided in the genus *Celoporthe*, with *Celoporthe* representing a distinct lineage in the Cryphonectriaceae (FIG. 2) (ML bootstrap = 63%).

The partition homogeneity test (PHT) comparing the exons in the *BT* gene region and the 5.8S rRNA gene datasets gave a PHT value of $P = 0.988$, indicating that these two datasets do not have a significant conflict and could be combined in the phylogenetic analyses. The aligned sequences of the combined datasets consisted of 61 taxa and 760 characters (TreeBASE: http://purl.org/phylo/treebase/phylows/study/TB2:S11111) (TABLE II). Similar to results of the LSU dataset, the position of the genera in relation to each other differed slightly based on the three different analyses, but the topology was similar for the genera. Results showed that all genera in the Cryphonectriaceae resided in discrete clades with high support values in at least one of the three analyses (FIG. 3). Only one most parsimonious tree was obtained (FIG. 3). Based on the phylogenetic analyses of the combined *BT* exons and 5.8S gene sequences, the isolates from *Eucalyptus* and *Syzygium* trees in China and Indonesia grouped closely with those of *C. dispersa* and separately from other genera in the Cryphonectriaceae (MP bootstrap = 87%, ML bootstrap = 89%, Bayesian posterior probabilities = 100%) (FIG. 3). Within the *Celoporthe* clade the isolates from Asia (China and Indonesia) formed several clades separate from that representing *C. dispersa* from South Africa (MP bootstrap = 92%, ML bootstrap = 71%, Bayesian posterior probabilities = 99%) (FIG. 3).

Species identification. The LSU phylogenetic analyses and BLAST queries for the *BT* and ITS gene sequences showed that the isolates considered in this study were phylogenetically most closely related to *Celoporthe* spp. The type species of this genus, *C. dispersa* (Nakabonge et al. 2006a), and *Celoporthe* isolates (CMW10779, CMW10780, CMW10781) collected from *S. aromaticum* trees in Indonesia (Myburg et al. 2003, Nakabonge et al. 2006a) were included with the isolates collected from China for species identification. The partition homogeneity test (PHT) comparing the *BT*, ITS and *TEF-1*α datasets gave a PHT value of $P = 0.998$, indicating that these three datasets do not have a significant conflict and could be combined for phylogenetic analyses. This was supported by the topologies of the separate trees of the three gene datasets and the combination datasets that consistently showed the same phylogenetic groups (FIG. 4A–C).

Where the three datasets (TreeBASE: http://purl.org/phylo/treebase/phylows/study/TB2:S11111) were analyzed separately, four equally most parsimonious trees were obtained for the two *BT* gene regions (FIG. 4A) while one most parsimonious tree was obtained respectively for the ITS (FIG. 4B) and *TEF-1*α (FIG. 4C) datasets. Results for all three gene regions showed that the Asian isolates are distinct from *C. dispersa*, with long phylogenetic branch distances and high support values (branch distances 17–42; MP bootstrap value 100% for each of the three genes) (FIG. 4A–C). The phylogenetic analyses for each of the *BT*, ITS and *TEF-1*α gene regions further showed that the Asian isolates formed four clades supported by long phylogenetic branch distances and high support values (branch distances up to 6; MP bootstrap value up to 100%; ML bootstrap value up to 99%; Bayesian posterior probabilities up to 100%). In these clades isolates (CMW24912, CMW24914, CMW24917, CMW34023, CMW34024) from *S. cumini* trees in China formed a single clade, isolates (CMW26900, CMW26908, CMW-26911, CMW26913) from a Chinese *Eucalyptus* clone formed a second clade, one isolate (CMW12750) from a Chinese *Eucalyptus* sp. resided in a third clade and isolates (CMW10779, CMW10780, CMW10781) from *S. aromaticum* trees in Indonesia formed the fourth (FIG. 4A–C).

Single nucleotide polymorphism (SNP) analyses supported the distinction of four clades for the Asian (Chinese and Indonesian) *Celoporthe* isolates considered in this study. Unique SNPs could be identified for all four phylogenetic groups for each of the gene regions sequenced (TABLES III, IV). Comparisons of the three gene regions showed that each clade was separated from the other three clades by 4–11 unique SNPs for each gene region (TABLE III). The total number of SNP differences between the four clades for all three gene regions combined varied between 21–31 unique SNPs (TABLE IV). No nucleotide differences could be detected in the *BT*, ITS and *TEF-1*α gene regions for the isolates within each of the three Chinese *Celoporthe* clades. In the Indonesian *Celoporthe* clade some nucleotide differences in the *BT* (10 bp) and ITS (12 bp) regions were found between isolate CWM10780 and the other two (CMW10781, CMW10779) isolates. This could not be confirmed for sequence data of the *TEF-1*α gene region because these cultures (CMW10779, CWM10780) are dead.

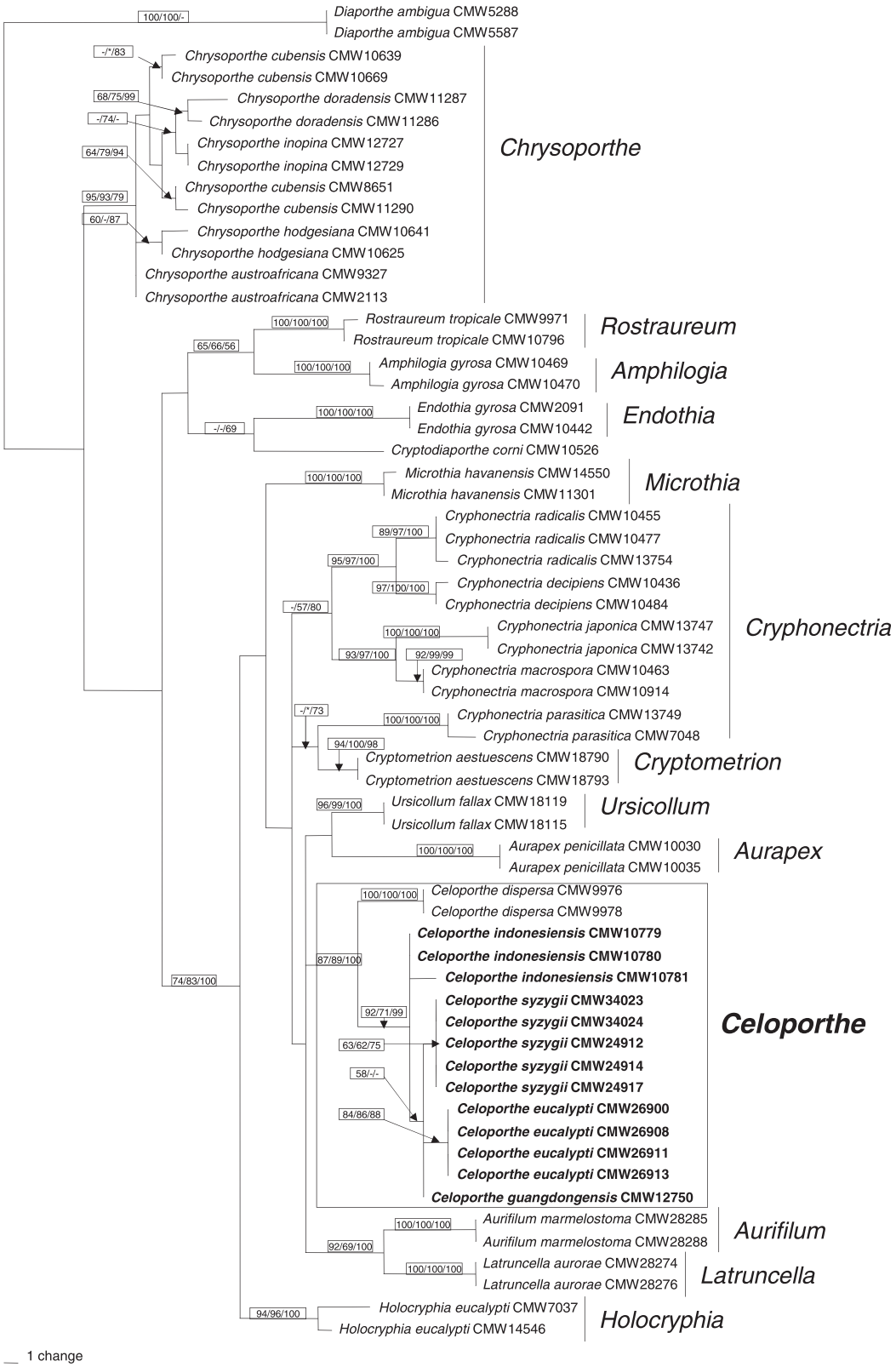

FIG. 3. Cladogram based on maximum parsimony (MP) analysis of a combined DNA sequence dataset of gene regions of the the partial exon 4, exon 5, partial exon 6 and partial exon 7 of the *BT* genes, and the *5.8S* rRNA gene region. Bootstrap values > 50% for MP and maximum likelihood (ML), and posterior probabilities > 70% obtained from Bayesian anlyses are presented above branches as follows: MP/ML/Bayesian. Bootstrap values lower than 50%, posterior probabilities lower than 70% are marked with *, and analysis value absent is marked with −. Two isolates of *Diaporthe ambigua* (CMW5587, CMW5288) represent the outgroup.

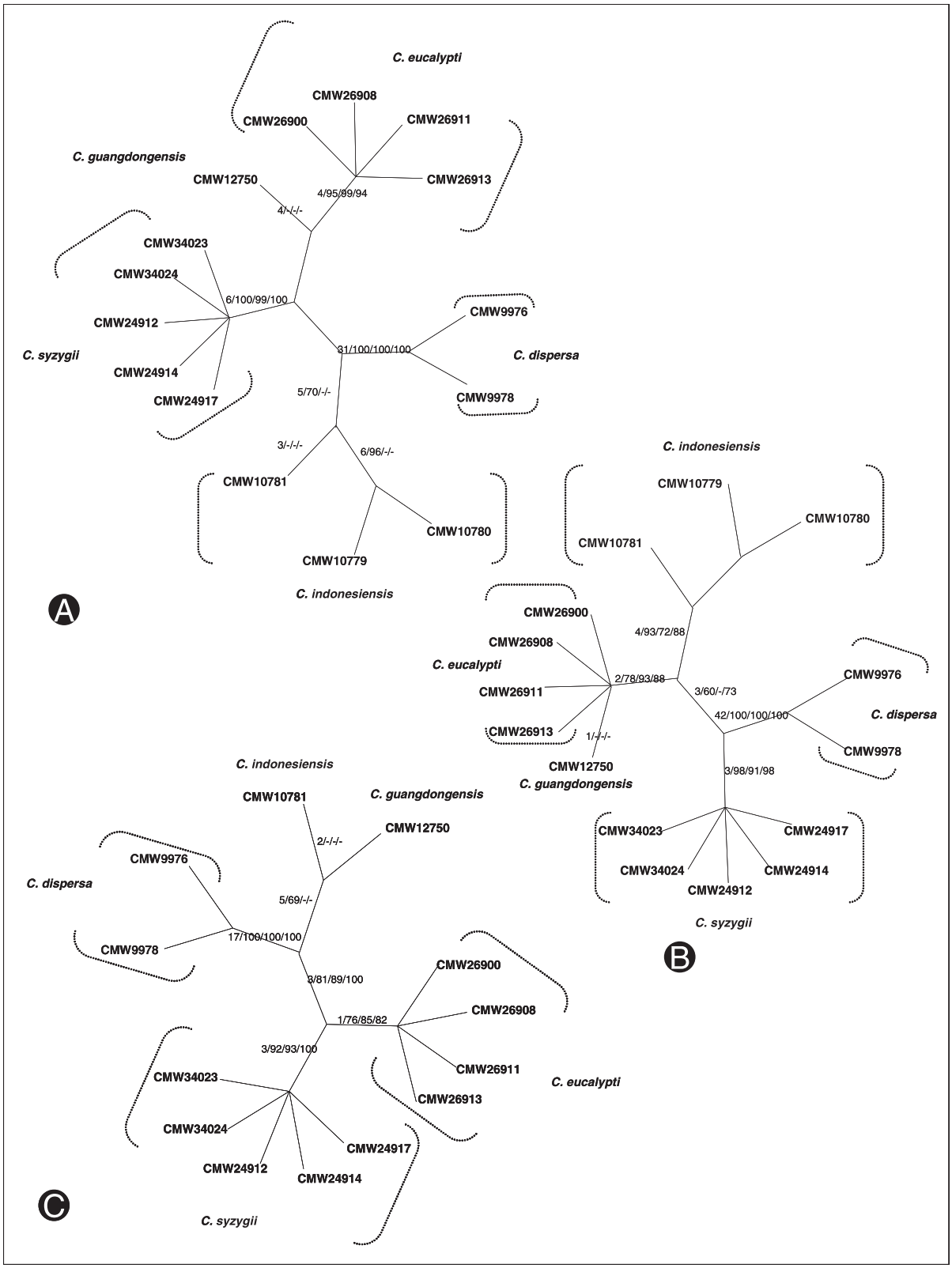

FIG. 4. Unrooted phylogenetic tree obtained with parsimony from DNA sequence datasets of three gene regions. A. *BT* gene region (*BT1* and *BT2*). B. ITS (ITS1, ITS2 and 5.8S rRNA) region. C. *TEF-1α* gene region. Branch length (BL), bootstrap values > 50% for MP and Maximum likelihood (ML), and posterior probabilities > 70% obtained from Bayesian anlyses are presented above branches as follows: BL/MP/ML/Bayesian. Bootstrap values lower than 50%, posterior probabilities lower than 70% are marked with *, and analysis value absent is marked with −.

TABLE III. Summary of polymorphic nucleotides found within the *BT* (*1* and *2*), ITS and the partial *TEF-1α* gene regions generated for the phylogenetic groups of *Celoporthe syzygii*, *C. eucalypti*, *C. guangdongensis* and *C. indonesiensis*

Species	Isolate number	*BT1*[a]								*BT2*									
		71[b]	119	141	188	189	192	194	202	24	223	233	234	235	236	237	238	241	327
C. syzygii	CMW34023	C	G	**T**[c]	C	T	C	C	**A**	C	**A**	C	C	—	—	C	C	**G**	**A**
	CMW34024	C	G	**T**	C	T	C	C	**A**	C	**A**	C	C	—	—	C	C	**G**	**A**
	CMW24912	C	G	**T**	C	T	C	C	**A**	C	**A**	C	C	—	—	C	C	**G**	**A**
	CMW24914	C	G	**T**	C	T	C	C	**A**	C	**A**	C	C	—	—	C	C	**G**	**A**
	CMW24917	C	G	**T**	C	T	C	C	**A**	C	**A**	C	C	—	—	C	C	**G**	**A**
C. eucalypti	CMW26900	C	**A**	C	C	T	**T**	C	C	**T**	C	C	T	—	—	—	C	C	C
	CMW26908	C	**A**	C	C	T	**T**	C	C	**T**	C	C	T	—	—	—	C	C	C
	CMW26911	C	**A**	C	C	T	**T**	C	C	**T**	C	C	T	—		—	C	C	C
	CMW26913	C	**A**	C	C	T	**T**	C	C	**T**	C	C	T	—	—	—	C	C	C
C. guangdongensis	CMW12750	**T**	G	C	**T**	**C**	C	**T**	C	C	C	—	—	—	—	—	C	C	C
C. indonesiensis	CMW10779	C	G	C	C	T	C	C	C	C	C	C	C	**T**	**T**	C	**T**	C	C
	CMW10780	C	G	C	C	T	C	C	C	C	C	C	C	**T**	**T**	C	**T**	C	C
	CMW10781	C	G	C	C	T	C	C	C	C	C	C	C	**T**	**T**	C	**T**	C	C

[a] Polymorphic nucleotides occurring only in all isolates are shown, not alleles that partially occur in individuals per phylogenetic group.

[b] Numerical positions of the nucleotides in the DNA sequence alignments are indicated; numerical positions for the exon of BT and 5.8S rRNA region are shaded.

[c] Fixed polymorphisms for each group are shaded and in boldface, those fixed but shared between two groups are shaded only.

Morphology.—For the morphological examination of material linked the various phylogenetic groups arising from DNA sequence comparisons fruiting bodies of the teleomorph and anamorph states from natural infections were available only for the *S. cumini* isolates from southern China. The fungus on *S. cumini* trees in China was characterized by fruiting structures (FIG. 5) that are morphologically similar to those of *C. dispersa* (Nakabonge et al. 2006a). Both of their teleomorph states were characterized by short, extending, orange to umber, cylindrical perithecical necks (FIG. 5A), semi-immersed stromata (FIG. 5B) and hyaline ascospores with one median septum (FIG. 5G). For the anamorph conidiomata were pulvinate to conical without a prominent neck (FIG. 5H–J), orange when young (FIG. 5H) and fuscous-black when mature. Their conidiomatal base tissue was prosenchymatous (FIG. 5L), and paraphyses or cylindrical sterile cells were present (FIG. 5M). Cultures were fluffy with uneven margins and white when young. A number of differences between *C. dispersa* and the specimens from *S. cumini* were visible. Asci of the fungus from *S. cumini* (av. 34.0 × 6.0 μm) were longer than those of *C. dispersa* (av. 26.5 × 6.3 μm). The conidiomatal locules in the *S. cumini* specimens were multilocular, seldom unilocular, while the structures of *C. dispersa* were unilocular, seldom multilocular. The conidia of the *S. cumini* specimens (av. 3.0 × 1.2 μm) were smaller than those of *C. dispersa* (av. 3.5 × 1.5 μm). Cultures of the fungus from *S. cumini* turned yellow-white to sulfur yellow with sienna/umber patches, while those of *C. dispersa* turned umber to hazel to chestnut with gray patches (Nakabonge et al. 2006a).

Due to the unavailibility of naturally infected tissue representing all four clades from Asia, fruiting structures produced on inoculated branch sections of *S. cordatum* and the *E. grandis* clone after 6 mo were used to determine morphological differences among the fungi in the clades. For the branch sections where both ends were coated with melted paraffin abundant anamorph structures covered the surface of the bark (FIG. 1C, D). For the branch sections where only the top ends were coated substantially fewer anamorph structures were produced. No teleomorph structures were produced on any of the inoculated branch sections.

Fruiting structures produced on the inoculated branch stubs were similar to those on naturally infected tissue, except for some variations in the shape, size and position of conidiomata (FIGS. 5, 6). For isolates in the same phylogenetic groups fruiting structures on the inoculated *S. cordatum* and *E. grandis* branch sections were similar in terms of conidiomatal position, shape, color and tissue tape making up the conidiomata, structure of conidiomatal locules, as well as shape and size of conidiophores, conidiogenous cells, paraphyses and conidia. Only the conidiomata on *S. cordatum* were larger than

TABLE III. Continued

ITS															*TEF-1α*												
40	82	84	85	92	93	97	100	118	132	180	181	211	212	489	35	47	48	76	128	129	138	214	215	230	234	240	249
C	T	—	—	T	C	T	C	C	—	—	—	—	A	—	C	T	T	A	T	T	A	—	—	A	G	T	T
C	T	—	—	T	C	T	C	C	—	—	—	—	A	—	C	T	T	A	T	T	A	—	—	A	G	T	T
C	T	—	—	T	C	T	C	C	—	—	—	—	A	—	C	T	T	A	T	T	A	—	—	A	G	T	T
C	T	—	—	T	C	T	C	C	—	—	—	—	A	—	C	T	T	A	T	T	A	—	—	A	G	T	T
C	T	—	—	T	C	T	C	C	—	—	—	—	A	—	C	T	T	A	T	T	A	—	—	A	G	T	T
C	T	—	—	C	T	C	G	—	G	A	—	—	—	—	T	G	C	A	T	T	A	—	—	A	G	T	T
C	T	—	—	C	T	C	G	—	G	A	—	—	—	—	T	G	C	A	T	T	A	—	—	A	G	T	T
C	T	—	—	C	T	C	G	—	G	A	—	—	—	—	T	G	C	A	T	T	A	—	—	A	G	T	T
C	T	—	—	C	T	C	G	—	G	A	—	—	—	—	T	G	C	A	T	T	A	—	—	A	G	T	T
C	T	—	—	C	T	C	G	C	G	A	A	—	—	T	C	G	C	A	—	—	C	A	—	G	A	C	C
T	A	T	A	C	T	C	G	—	G	—	—	A	A	—													
T	A	T	A	C	T	C	G	—	G	—	—	A	A	—													
T	A	T	A	C	T	C	G	—	G	—	—	A	A	—	C	G	C	G	—	—	C	A	C	A	A	T	T

those on *E. grandis* (FIGS. 6–9). Similar differences were observed by Hodges et al. (1986) who inoculated excised branch stubs to produce fruiting structures.

The four Asian phylogenetic clades of *Celoporthe* could be distinguished from *C. dispersa* based on morphological characteristics observed on the limited naturally infected tissue as well as on the artificially inoculated branch pieces. The conidiomata of *C. dispersa* are usually unilocular (TABLE V) (Nakabonge et al. 2006a), while the conidiomata of isolates in all Asian clades were predominantly multilocular (TABLE V, FIGS. 5–9). The paraphyses of *C. dispersa* were shorter than those for all the isolates in the Asian clades (TABLE V). Last, the naturally infected bark from *S. cumini* trees showed that the asci of *C. dispersa* are much shorter than those of the Asian isolates (TABLE V). The four Asian phylogenetic clades of *Celoporthe* also could be distinguished from *C. dispersa* based on growth characteristics in culture. The optimal temperature for the growth of *C. dispersa* was 25 C (Nakabonge et al. 2006a), while that for isolates in all of the Asian *Celoporthe* clades was 30 C.

Isolates representing the four Asian clades of *Celoporthe* could be destinghuished based on several morphological features, including length of conidiophores and especially conidial shape and sizes as well as the length of paraphyses (TABLE V; FIG. 10A, B). Lengths of the paraphyses ($P < 0.01$ to $P = 0.018$) differed between isolates for each of the four Asian clades. Except for conidial length between isolates of the two clades from the Chinese *Eucalyptus* clone and a *Eucalyptus* species ($P = 0.74$), length of the conidia ($P < 0.01$) was significantly different for isolates representing the four Asian clades (FIG. 10A, B). For example the conidia of isolates in the Indonesian *Celoporthe* clade were the longest ($P < 0.01$) of all isolates in the four Asian clades while the paraphyses of these isolates were shorter ($P < 0.01$ to $P = 0.018$) than those of isolates in the two Chinese *Celoporthe* clades from *Eucalyptus* trees (TABLE V; FIG. 10A, B).

TAXONOMY

Based on phylogenetic analyses, the Asian isolates characterized in this study reside in the genus *Celoporthe*. These isolates could be divided into four phylogenetic clades, separate from that of the type species, *C. dispersa*. These clades and *C. dispersa* also could be distinguished from each other, based on characteristics of the asci, conidiomata, conidiophores, conidia, paraphyses and growth in culture.

TABLE IV. Number of unique alleles between *Celoporthe syzygii*, *C. eucalypti*, *C. guangdongensis* and *C. indonesiensis*

BT1/2/ITS/*TEF-1α*[a]	*C. eucalypti*	*C. guangdongensis*	*C. indonesiensis*
C. syzygii	21 (10/8/3)	31 (12/9/10)	29 (9/11/9)
C. eucalypti		21 (9/3/9)	24 (9/7/8)
C. guangdongensis			26 (11/10/5)

[a] The order of the three genes: *BT*, ITS and *TEF-1α*.

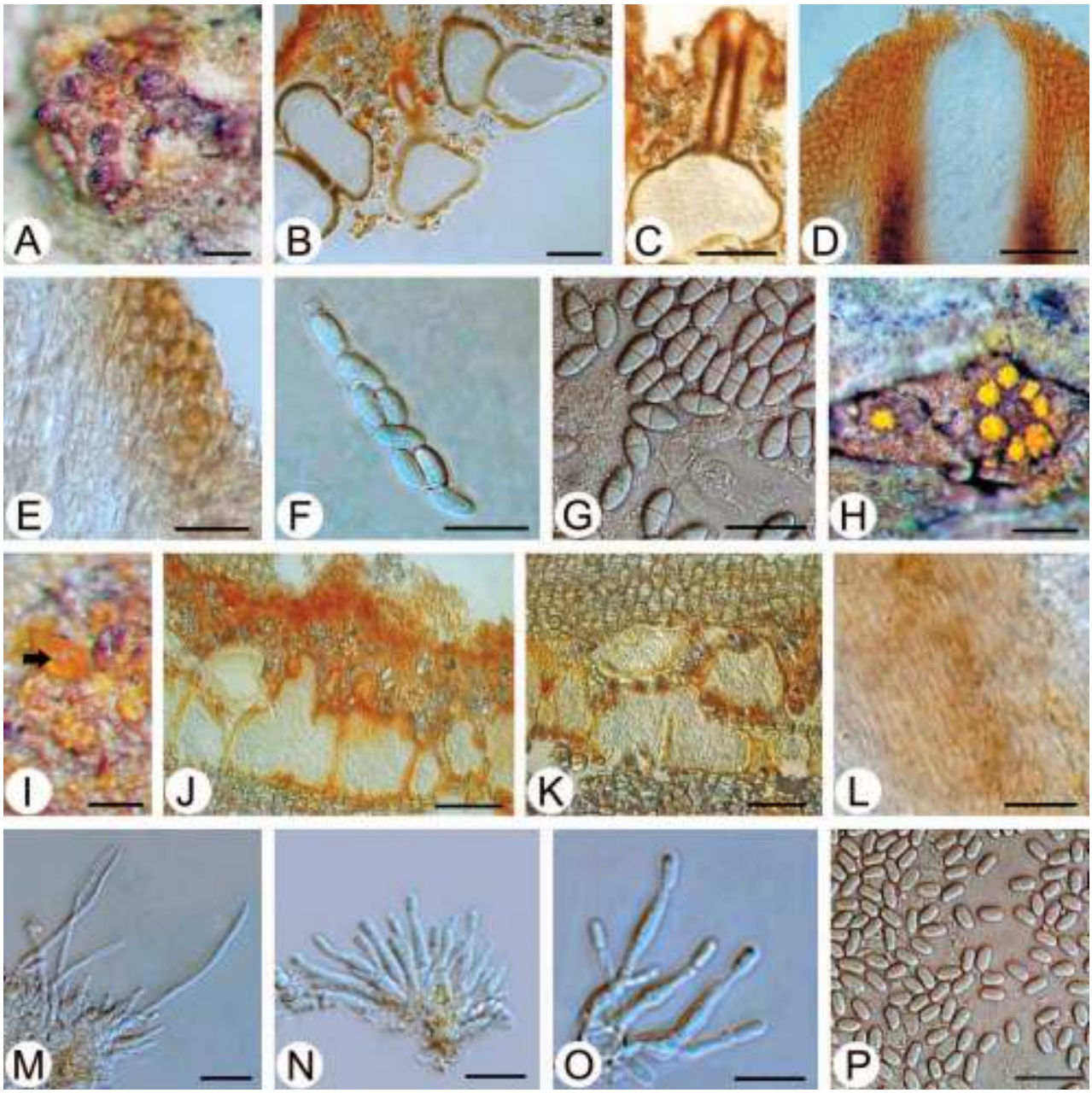

FIG. 5. Fruiting structures of *C. syzygii* on natural *S. cumini* trees. A. Ascostroma on bark. B, C. Longitudinal section through ascostroma. D. Perithecial neck tissue. E. Stromatic tissue of ascostroma. F. Ascus with ascospores. G. Ascospores. H, I. Conidomata on the bark (arrow indicate conidial spore mass). J. Longitudinal section through conidioma. K. Latitudinal section through conidioma. L. Stromatic tissue of conidioma. M. Paraphyses. N, O. Conidiophores and conidigenous cells. P. Conidia. Bars: A–C, I–K = 100 μm; H = 200 μm; D = 20 μm; E–G, L–P = 10 μm.

The Asian isolates therefore represent four distinct species and are described as follows:

Celoporthe syzygii S.F. Chen, Gryzenh., M.J. Wingf. & X.D. Zhou, sp. nov. FIGS. 5, 6
MycoBank MB519066

Etymology. The name refers to the fact that the species was isolated from *Syzygium* trees.

Asci fusoidei (29.5–)31.5–36.5(–43) × (5–)5.5–6.5(–7) μm. Ascosporae oblongo-ellipsoideae (5–)6–7.5(–8.5) × 2.5–3(–3.5) μm. Loculi conidiomatum multiloculares raro uniloculares. Conidiophorae (4.5–)6.0–11.0(–16.0) μm longae. Paraphyses usque ad 52 μm. Conidia oblonga vel cylindrica raro allantoidea, (2.3–)2.8–3.4(–3.8) × (1.0–)1.3(–1.6) μm. A speciebis aliis cladi asiatici Celoporthis (*C. eucalypti*, *C. guangdongensis*, *C. indonesiensis*) nucleotidis unice fixis in tribus locis nuclearibus differt: β-tubulinum-1

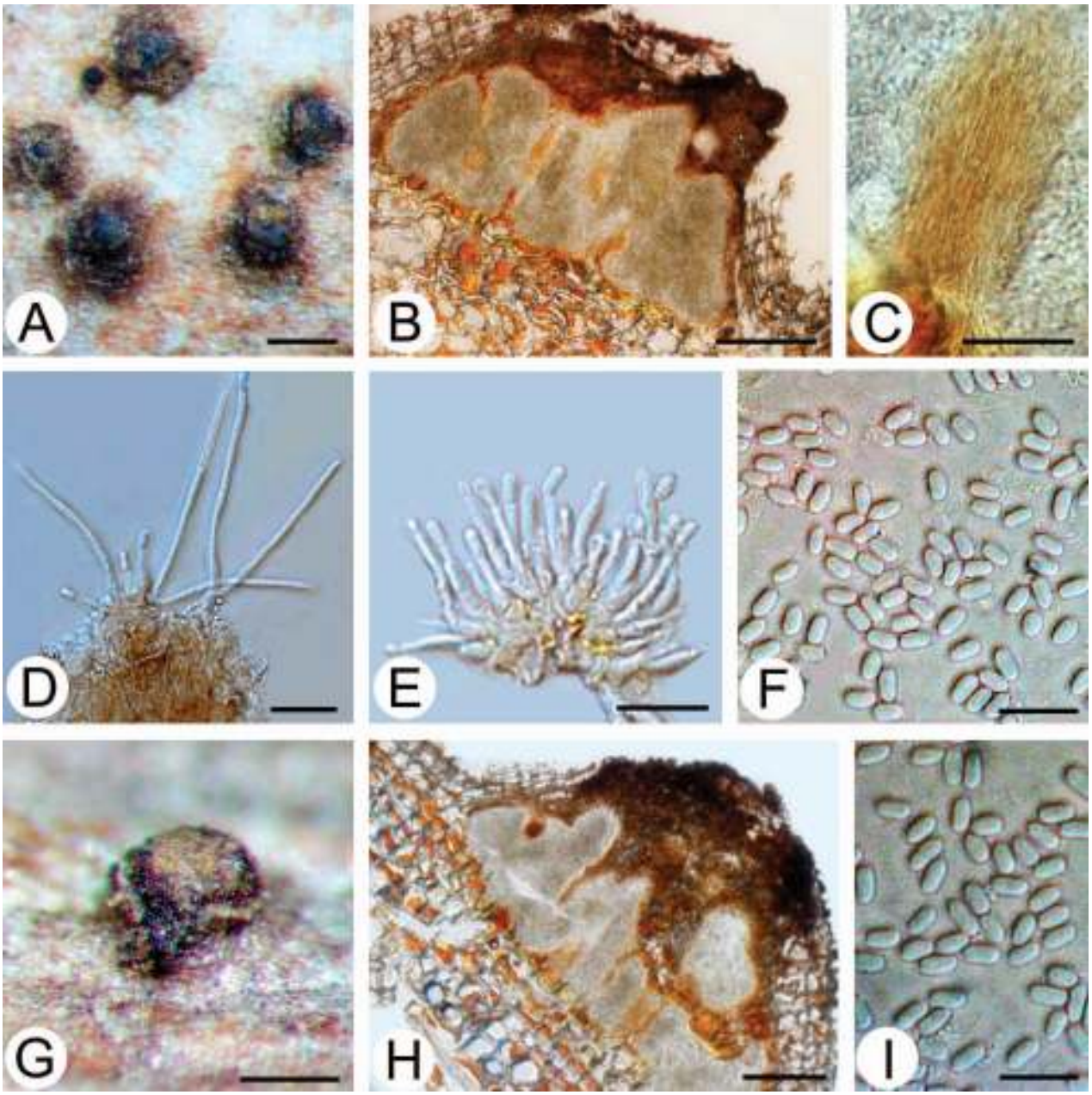

FIG. 6. Fruiting structures of *C. syzygii* on inoculated branch tissue of *S. cordatum* (A–F) and an *E. grandis* clone (G–I). A, G. Conidiomata on the bark. B, H. Longitudinal section through conidioma. C. Stromatic tissue of conidioma. D. Paraphyses. E. Conidiophores and conidigenous cells. F, I. Conidia. Bars: A, B, G, H = 100 μm; C = 20 μm; D–F, I = 10 μm.

sitis 141 (T), 202 (A); β-tubulinum-2 sitis 223 (A), 241 (G), 327 (A), loco vulgo ''internal transcribed spacer rDNA'' dicto (ITS1, 5.8S et ITS2) sitis 92 (T), 93 (C), 97 (T), 100 (C) et 132 (–) et loco vulgo ''translation elongation factor 1-alpha'' dicto sitis 47 (T) et 48 (T).

Ascostromata on the bark taken from cankers on *S. cumini* trees gregarious, seldom single, immersed or semi-immersed; recognizable by short, extending, umber, cylindrical perithecial necks, occasionally erumpent, limited; orange to umber ascostromatic tissue covering the tops of the perithecial bases; ascostromata 40–240 μm (av. 120 μm) high above the level of bark and 280–580 μm (av. 300 μm) wide above the surface of the bark (FIG. 5A). Stromatic tissue pseudoparenchymatous at the edges, prosenchymatous in the center (FIG. 5E). Perithecia valsoid, 1–15 per stroma; bases immersed in the bark, black, globose to subglobose, 60–380 μm (av. 170 μm) diam; perithecial wall 10–35 μm (av. 18 μm) thick (FIG. 5B, C); perithecial necks black, emerging through the

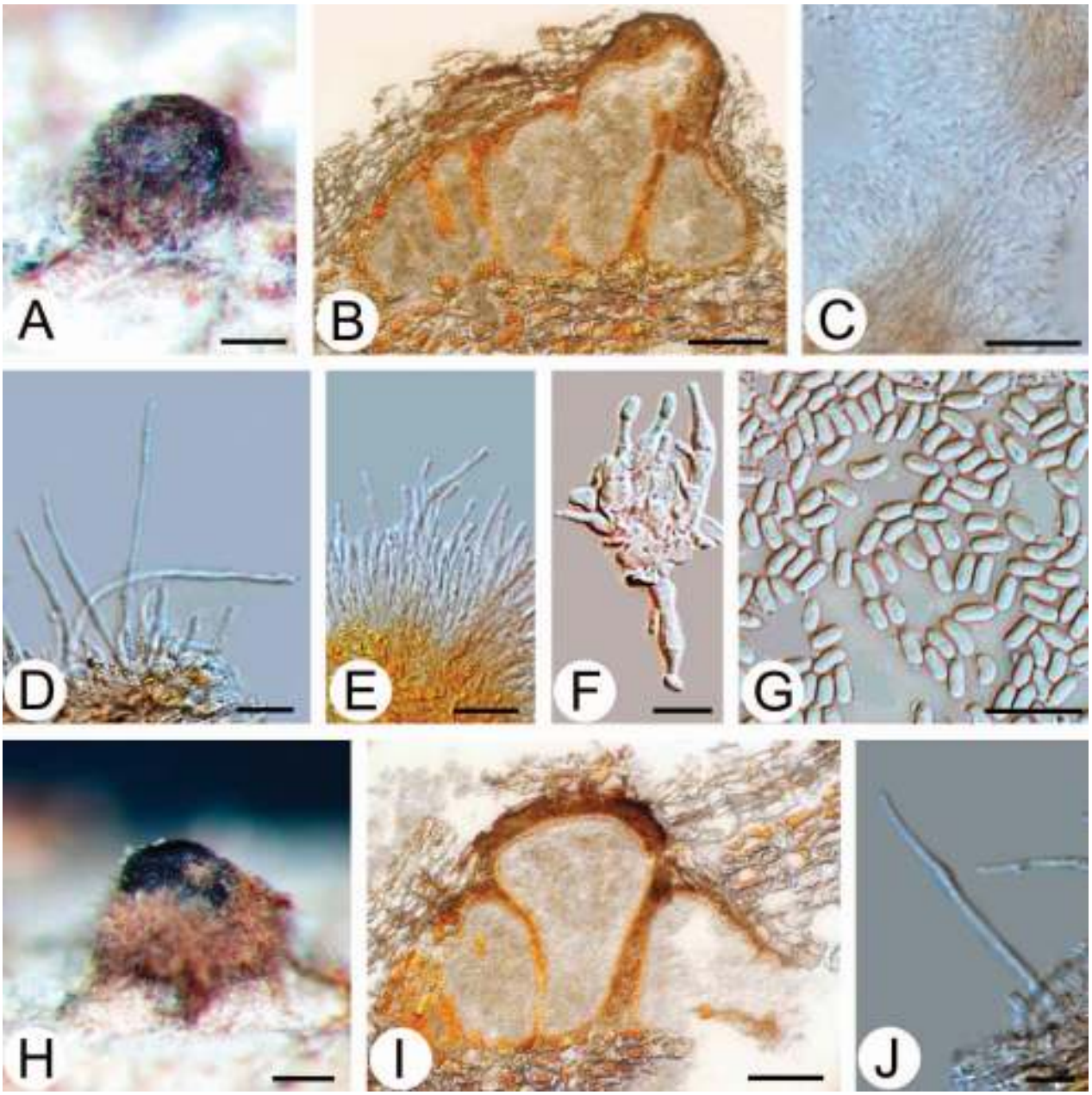

FIG. 7. Fruiting structures of *C. eucalypti* on inoculated branch tissue of an *E. grandis* clone (A–G) and *S. cordatum* (H–J). A, H. Conidiomata on the bark. B, I. Longitudinal section through conidioma. C. Stromatic tissue of conidioma. D, J. Paraphyses. E, F. Conidiophores and conidigenous cells. G. Conidia. Bars: A, B, H, I = 100 μm; C = 20 μm; D–G, J = 10 μm.

stromatal surface, covered in orange to umber stromatic tissue of textura porrecta (FIG. 5D), necks emerge at stromatal surface as black ostioles covered with umber to brown stromatal tissue to form papillae extending up to 40 μm long, 40–90 μm (av. 55 μm) wide (FIG. 5C). Asci eight-spored, biseriate, unitunicate, free when mature, non-stipitate with a non-amyloid refractive ring, fusoid, (29.5–)31.5–36.5(–43) × (5–)5.5–6.5(–7) μm (FIG. 5F). Ascospores hyaline, with one median septum, oblong-ellipsoidal, with rounded ends, (5–)6–7.5(–8.5) × 2.5–3(–3.5) μm (FIG. 5G).

Conidiomata part of ascomata as conidial locules or as solitary structures; immersed to semi-immersed to superficial; pulvinate without necks, occasionally with a neck that is attenuated, orange when young, umber to brown to fuscous-black when mature; conidiomatal base 90–300 μm (av. 170 μm) high above the level of bark and 180–900 μm (av. 420 μm) wide above the surface of the bark (FIG. 5H, I). Conidiomatal locules

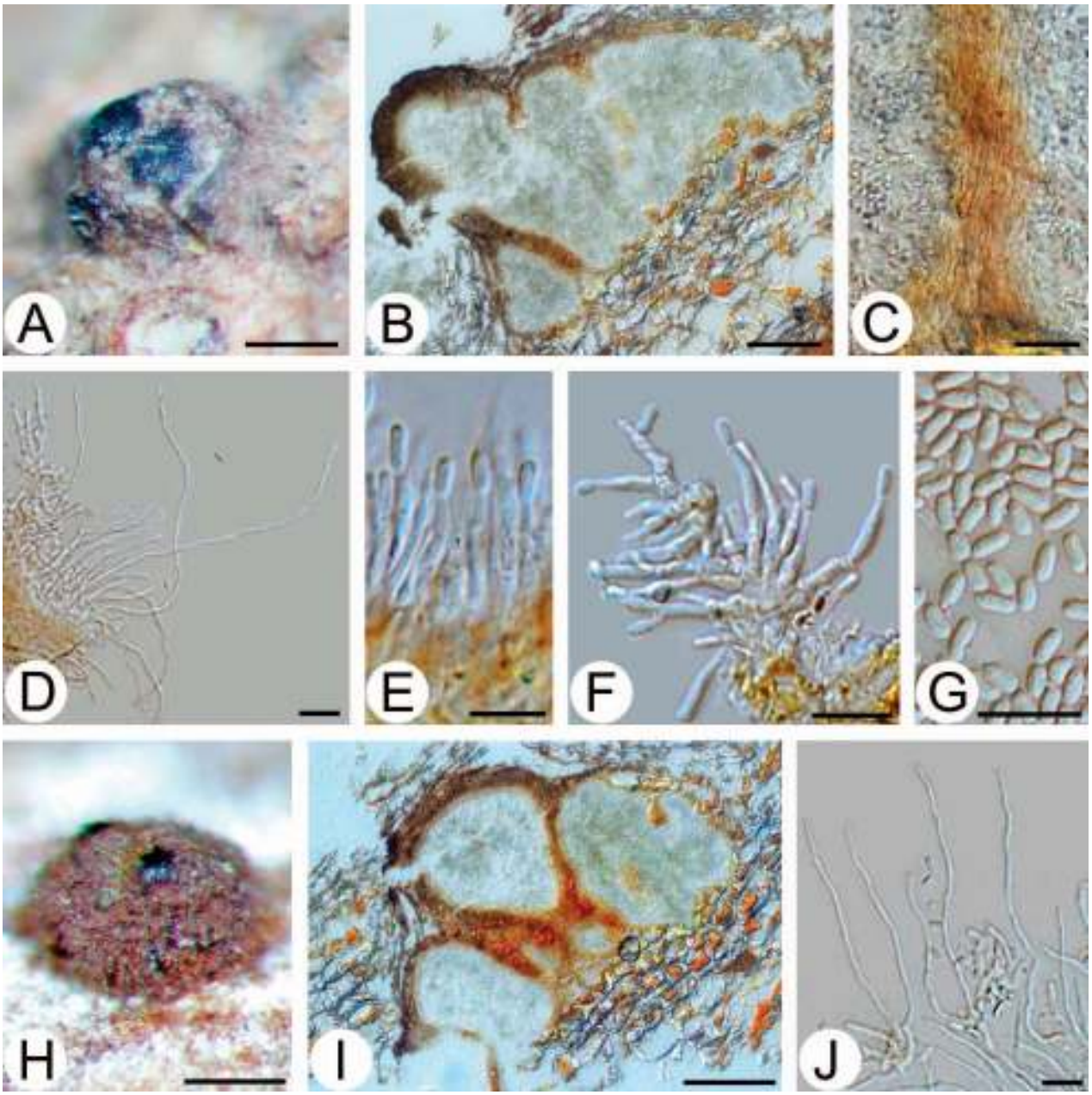

FIG. 8. Fruiting structures of *C. guangdongensis* on inoculated branch tissue of an *E. grandis* clone (A–G) and *S. cordatum* (H–J). A, H. Conidiomata on the bark. B, I. Longitudinal section through conidioma. C. Stromatic tissue of conidioma. D, J. Paraphyses. E, F. Conidiophores and conidigenous cells. G. Conidia. Bars: A, B, H, I = 100 μm; C = 20 μm; D–G, J = 10 μm.

multilocular, seldom unilocular, locules 50–650 μm (av. 260 μm) diam (FIG. 5J, K). Stromatic tissue of base prosenchymatous (FIG. 5L). Conidiophores hyaline, branched irregularly at the base or above into cylindrical cells, with or without separating septa, (4.5–)6.0–9.0(–12.5) μm (av. 8.0 μm) long (FIG. 5N, O). Conidiogenous cells phialidic, cylindrical with or without attenuated apices, 1.0–2.0(–2.5) μm (av. 2.0 μm) wide (FIG. 5N, O). Paraphyses or cylindrical sterile cells occur among conidiophores, up to 44 μm long (av. 17 × 1.5 μm) (FIG. 5M). Conidia hyaline, non-septate, oblong to cylindrical, occasionally allantoid, pushed through opening at stromatal surface as orange droplets (FIG. 5I), (2.3–)2.8–3.3(–3.7) × (1.0–)1.1–1.3(–1.5) μm (av. 3.0 × 1.2 μm) (FIG. 5P).

No ascostroma were observed on either inoculated *S. cordatum* or *E. grandis* branch tissue. The inoculated material on both the *S. cordatum* and *E. grandis* branch tissue was similar in morphology to the structures on field-collected *S. cumini* bark

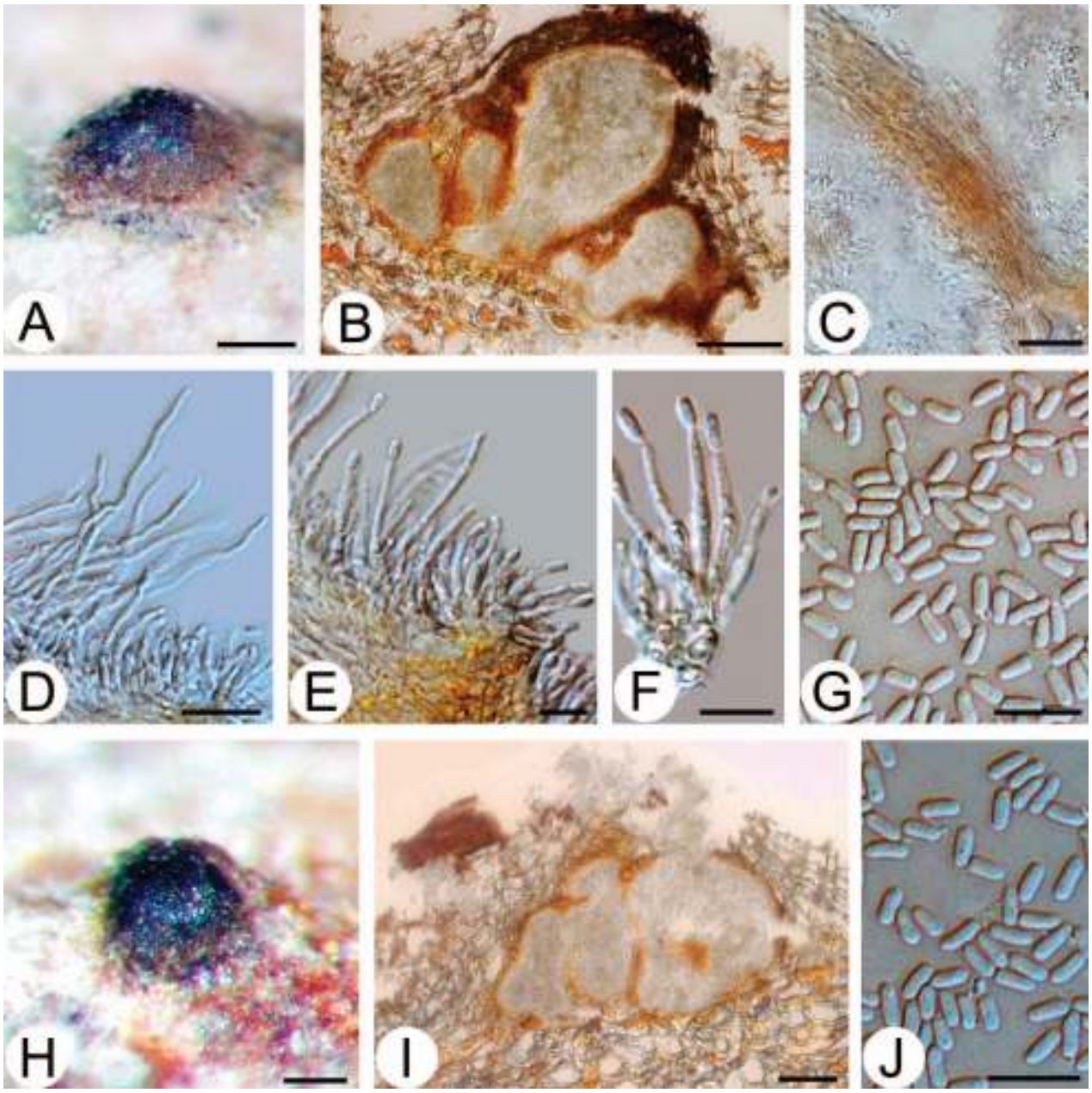

FIG. 9. Fruiting structures of *C. indonesiensis* on inoculated branch tissue of *S. cordatum* (A–G) and an *E. grandis* clone (H–J). A, H. Conidiomata on the bark. B, I. Longitudinal section through conidioma. C. Stromatic tissue of conidioma. D. Paraphyses. E, F. Conidiophores and conidigenous cells. G, J. Conidia. Bars: A, B, H, I = 100 μm; C = 20 μm; D–G, J = 10 μm.

(FIGS. 5, 6). However *conidiomata* on inoculated *S. cordatum* and *E. grandis* branches were eustromatic, superficial to slightly immersed (FIG. 6B, H); conidiomatal base on *S. cordatum* 100–400 μm (av. 160 μm) high above the level of bark and 200–700 μm (av. 320 μm) wide above the surface of bark (FIG. 6A); on *E. grandis* 80–280 μm (av. 140 μm) high above the level of bark and 140–620 μm (av. 290 μm) wide above the surface of bark (FIG. 6G). Conidiomatal locules on *S. cordatum* 70–540 μm (av. 250 μm) diam (FIG. 6B), on *E. grandis* 40–490 μm (av. 240 μm) diam (FIG. 6H). Paraphyses or cylindrical sterile cells on *S. cumini* branches up to 42 μm long (av. 18 × 1.5 μm) (FIG. 6D), on *E. grandis* branches up to 52 μm long (av. 24 × 1.5 μm).

Celoporthe syzygii differs from other species in the Asian clade of *Celoporthe* (*C. eucalypti*, *C. guangdongensis*, *C. indonesiensis*) by uniquely fixed DNA nucleotides in three nuclear loci, *BT1* positions 141 (T) and 202 (A), *BT2* positions 223 (A), 241 (G) and

327 (A); ITS (ITS1, 5.8S, ITS2) positions 92 (T), 93 (C), 97 (T), 100 (C) and 132 (–); *TEF-1α* positions 47 (T) and 48 (T).

Culture characteristics. On MEA *C. syzygii* fluffy with an uneven margin, white when young, turning yellow white to sulfur yellow with sienna/umber patches after 10 d. Colony reverse white to yellow-white. Optimal growth temperature 30 C, covering the 90 mm plates after 5 d. No growth at 5 C and 35 C; colonies at 10 C reached 31.5 mm in 30 d (6 mm in 7 d). Asexual fruiting structures occasionally form in primary isolations of the fungus.

Substrate. Bark of *Syzygium cumini*.

Distribution. China.

Specimens examined. CHINA, GUANGDONG PROVINCE, *S. cumini*. Sep 2008, *S.F. Chen*, HOLOTYPE PREM 60462, EX-TYPE culture CMW34023 = CBS127218; PARATYPE PREM 60463, living culture CMW34024; Dec 2006, *M.J. Wingfield & X.D. Zhou*, PARATYPE PREM 60464 (isolate CMW24912 = CBS127188, artificial inoculation on South African *S. cordatum* and *E. grandis* branch tissue in Apr 2008, *S.F. Chen*); Dec 2006, *M.J. Wingfield & X.D. Zhou*, PARATYPE PREM 60465 (isolate CMW24914 = CBS127189, artificial inoculation on South African *S. cordatum* and *E. grandis* branch tissue in Apr 2008, *S.F. Chen*).

Notes. *Celoporthe syzygii* is morphologically distinguishable from *C. dispersa* by having longer asci (av. 34 × 6 μm, L/W = 5.7) than *C. dispersa* (av. 26 × 6.3 μm, L/W = 4.1). The inoculated conidiomata of *C. syzygii* are more superficial than those of structures formed in nature. The conidia of *C. syzygii* (2.3–3.8 μm) are shorter than those of *C. guangdongensis* (2.4–4.3 μm), *C. eucalypti* (2.6–4.4 μm), *C. indonesiensis* (3.1–4.7 μm) and *C. dispersa* (2.5–5.5 μm).

Celoporthe eucalypti S.F. Chen, Gryzenh., M.J. Wingf. & X.D. Zhou, sp. nov. FIG. 7.
MycoBank MB519067

Etymology. Name refers to *Eucalyptus*, the host from which this fungus first was collected.

Loculi conidiomatum multiloculares raro uniloculares. Conidiophorae (4.5–)9.0–14.0(–25.0) μm longae. Paraphyses usque ad 68 μm. Conidia (2.6–)3.1–3.8(–4.4) × (1.1–)1.4–1.6(–1.8) μm. A speciebis aliis cladi asiatici Celoporthis (*C. syzygii, C. guangdongensis, C. indonesiensis*) nucleotidis unice fixis in duobus locis nuclearibus differt: β-tubulinum-1 sitis 119 (T) et 192 (T), β-tubulinum-2 sito 24 (T), et loco vulgo ''translation elongation factor 1-alpha'' dicto sito 35 (T).

No ascostromata were observed on either the field-collected *Eucalyptus* bark or on inoculated *S. cordatum* and *E. grandis* branch tissue. Both on *S. cordatum* and *E. grandis* the conidiomata on inoculated branch tissue were eustromatic, superficial to slightly immersed, pulvinate without necks, sometimes conical, orange to umber when young, fuscous-black when mature (FIG. 7A, H). Stromatic tissue of base prosenchymatous (FIG. 7C). However the conidiomatal base on *S. cordatum* 120–600 μm (av. 260 μm) high above the level of bark and 150–700 μm (av. 400 μm) wide above the surface of the bark (FIG. 7H), on *E. grandis* 100–410 μm (av. 210 μm) high above the level of bark and 140–650 μm (av. 340 μm) wide above the surface of the bark (FIG. 7A). Conidiomatal locules multilocular, seldom unilocular, locules on *S. cordatum* 50–510 μm (av. 240 μm) diam (FIG. 7I), locules on *E. grandis* 35–580 μm (av. 260 μm) diam (FIG. 7B). Conidiophores hyaline, branched irregularly at the base or above into cylindrical cells, with or without separating septa, on *S. cordatum* (5.5–)9.5–13.5(–22.5) μm (av. 12.0 μm) long (FIG. 7F), on *E. grandis* (4.5–)9.0–14.0(–25.0) μm (av. 12 μm) long (FIG. 7E). Conidiogenous cells phialidic (FIG. 7F), cylindrical with or without attenuated apices, on *S. cordatum* 1.5–2.5(–3.0) μm (av. 2.0 μm) wide, on *E. grandis* 1.5–3.0(–3.5) μm (av. 2.5 μm) wide (FIG. 7E). Paraphyses or cylindrical sterile cells occur among conidiophores, on *S. cordatum* up to 68 μm long (av. 44 × 1.7 μm) (FIG. 7J), on *E. grandis* up to 62 μm long (av. 40 × 1.6 μm) (FIG. 7D). Conidia hyaline, non-septate, oblong to cylindrical, occasionally allantoid, extend through opening at stromatal surface as orange droplets, on *S. cordatum* (2.6–)3.2–3.7(–4.1) × (1.2–)1.4–1.6(–1.8) μm, (av. 3.5 × 1.5 μm), on *E. grandis* (2.7–)3.1–3.8(–4.4) × (1.1–)1.5–1.7(–1.8) μm, (av. 3.5 × 1.6 μm) (FIG. 7G).

Celoporthe eucalypti differs from other species in the Asian clade of *Celoporthe* (*C. syzygii*, *C. guangdongensis*, *C. indonesiensis*) by uniquely fixed DNA nucleotides in two nuclear loci: *BT1* positions 119 (A) and 192 (T), *BT2* position 24 (T); *TEF-1α* position 35 (T).

Culture characteristics. On MEA *C. eucalypti* fluffy with an uneven margin, white when young, turning pale luteous to luteous after 10 d. Colony reverse sulfur yellow to pale luteous after 10 d. Optimal growth temperature 30 C, covering 90 mm plates after 6 d. No growth at 5 C and 35 C, colonies at 10 C reached 16 mm in 30 d (4 mm in 7 d). Asexual fruiting structures occasionally formed in primary isolations of the fungus.

Substrate. Bark of *Eucalyptus* clone.

Distribution. China.

Specimens examined. CHINA, GUANGDONG PROVINCE, *Eucalyptus* clone. Jan 2007, *X.D. Zhou & S.F. Chen*. HOLOTYPE PREM 60467 (isolate CMW26908, artificial inoculation on South African *S. cordatum* and *E. grandis* branch tissue in Apr 2008, *S.F. Chen*), EX-TYPE culture CMW26908 = CBS127190; PARATYPE PREM 60466 (isolate CMW26900, artificial inoculation on South African *S. cordatum* and *E. grandis* branch tissue in Apr 2008, *S.F. Chen*), EX-TYPE culture CMW26900 = CBS127191.

TABLE V. Comparison of morphological characteristics of five *Celoporthe* species

		C. dispersa	*C. syzygii*	*C. eucalypti*	*C. guangdongensis*	*C. indonesiensis*
Species collected from	country	South Africa	China	China	China	Indonesia
	host	*S. cordatum*	*S. cumini*	*Eucalyptus* clone	*Eucalyptus* sp.	*S. aromaticum*
Conidiomata	height	**300–500**[a]	**80–400 (av. 163)**	**100–600 (av. 235)**	**90–720 (av. 255)**	**60–260 (av. 110)**
(above the bark)	width	**200–1000**	**140–900 (av. 343)**	**140–700 (av. 370)**	**120–750 (av. 395)**	**100–550 (av. 225)**
Conidiomatal locules	uni- or multilocular	**unilocular, occasionally multilocular**	**multilocular, seldom unilocular**	**multilocular, seldom unilocular**	**multilocular, seldom unilocular**	**multilocular, seldom unilocular**
	diameter	**100–550**	**40–650 (av. 250)**	**35–580 (av. 250)**	**35–640 (av. 280)**	**35–610 (av. 295)**
Conidiophores	length	**(9.5–)12.0–17.0(–19.5) (av. 14.5)**	**(4.5–)6.0–11.0(–16.0) (av. 9.0)**	**(4.5–)9.0–14.0(–25.0) (av. 12.0)**	**(4.5–)10.0–16.0(–27.5) (av. 13.5)**	**(5.5–)12.0–18.0(–32.0) (av. 15.5)**
Conidiogenous cells	width	(1.5–)2.0–3.0	1.0–2.0(–2.5) (av. 2.0)	1.5–2.5(–3.5) (av. 2.2)	1.5–2.5(–3.5) (av. 2.0)	(1.0–3.5) (av. 2.2)
Paraphyses or sterile cells	length	**up to 39 (av. 20)**	**up to 52 (av. 20)**	**up to 68 (av. 42)**	**up to 91 (av. 55)**	**up to 50 (av. 27)**
Conidia	shape	oblong (to cylindrical), occasionally allantoid	oblong (to cylindrical), occasionally allantoid	oblong (to cylindrical), occasionally allantoid	oblong (to cylindrical), occasionally allantoid	cylindrical, occasionally oblong or allantoid
	length	(2.5–)3–4(–5.5) (av. 3.5)	(2.3–)2.8–3.4(–3.8) (av. 3.1)	(2.6–)3.1–3.8(–4.4) (av. 3.5)	(2.4–)3.1–3.9(–4.3) (av. 3.5)	(3.1–)3.5–4.2(–4.7) (av. 3.9)
	width	**(1.0–)1.5(–2.5) (av. 1.5)**	**(1.0–)1.3(–1.6) (av. 1.3)**	**(1.1–)1.4–1.6(–1.8) (av. 1.6)**	**(1.1–)1.3–1.7(–1.9) (av. 1.5)**	**(1.1–)1.2–1.5(–1.6) (av. 1.3)**
	length/width	2.3	2.5	2.2	2.3	3
Ascostromata	height	100–400	40–240 (av. 120)	n/a[b]	n/a	n/a
(above the bark)	width	320–505	280–580 (av. 300)	n/a	n/a	n/a
Perithecia	no. perithecia per ascostroma	**1–6**	**1–15**	n/a n/a	n/a n/a	n/a n/a
	diameter	100–300	60–380 (av. 170)	n/a	n/a	n/a
Perithecial necks	length	50	40	n/a	n/a	n/a
	width	100–150	40–90	n/a	n/a	n/a
Asci	shape	fusoid to ellipsoidal	Fusoid	n/a	n/a	n/a
	length	**(19.5–)23.5–29.5(–33.5) (av. 26.5)**	**(29.5–)31.5–36.5(–43) (av. 34.0)**	n/a n/a	n/a n/a	n/a n/a
	width	**(4.5–)5.5–7(–7.5) (av. 6.3)**	**(5–)5.5–6.5(–7) (av. 6.0)**	n/a	n/a	n/a
	length/width	**4.2**	**5.7**	n/a	n/a	n/a
Ascospores	shape	oblong ellipsoidal	oblong ellipsoidal	n/a	n/a	n/a
	length	**(4.5–)6–7(–8) (av. 6.5)**	**(5–)6–7.5(–8.5) (av. 6.8)**	n/a	n/a	n/a
	width	(2–)2.5–3(–3.5) (av. 2.8)	2.5–3(–3.5) (av. 2.8)	n/a	n/a	n/a
	length/width	2.3	2.4	n/a	n/a	n/a

[a] The measurements are in micrometers, and the distinctive characters are in boldface.
[b] n/a, not available.

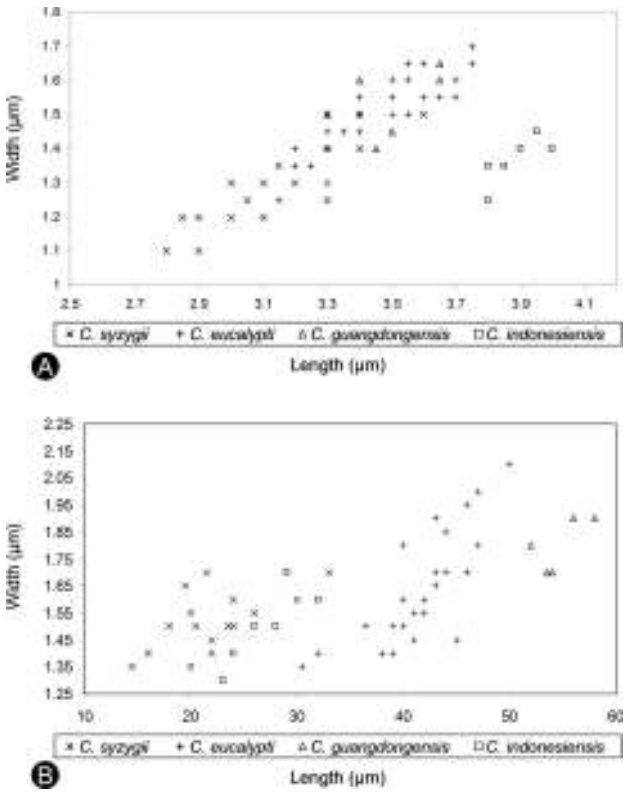

FIG. 10. The average lengths and widths of 10 conidia and 10 paraphyses measured for each of the inoculated *S. cordatum* and *E. grandis* branch stubs by four species of *Celoporthe*. A. Conidia. B. Paraphyses.

Notes. *Celoporthe eucalypti* is morphologically similar to *C. guangdongensis* but can be distinguished by having shorter paraphyses (up to 68 µm) than *C. guangdongensis* (up to 91 µm). *C. eucalypti* can be distinguished from *C. dispersa* (paraphyses up to 39 µm), *C. indonesiensis* (paraphyses up to 50 µm) and *C. syzygii* (paraphyses up to 52 µm) by its longer paraphyses. At 10 C on 2% MEA after 30 d *C. eucalypti* grew faster (av. colony diam = 16 mm) than *C. guangdongensis* (av. colony diam = 7 mm) and *C. indonesiensis* (av. colony diam = 1.5 mm) but slower than *C. syzygii* (av. colony diam. = 31.5 mm).

Celoporthe guangdongensis S.F. Chen, Gryzenh., M.J. Wingf. & X.D. Zhou, sp. nov. FIG. 8
MycoBank MB519068

Etymology. Name reflects the GuangDong Province of China where this fungus first was found.

Loculi conidiomatum multiloculares raro uniloculares. Conidiophorae (4.5–)10.0–16.0(–27.5) µm longae. Paraphyses usque ad 91 µm. Conidia (2.4–)3.1–3.9(–4.3) × (1.1–)1.3–1.7(–1.9) µm. A speciebis aliis cladi asiatici Celoporthis (*C. syzygii*, *C. guangdongensis*, *C. indonesiensis*) nucleotidis unice fixis in tribus locis nuclearibus differt: β-tubulinum-1 sitis 71 (T), 188 (T), 189 (C), 194 (T); β-tubulinum-2 sitis 233 (–) et 234 (–); loco vulgo ''internal transcribed spacer rDNA'' dicto (ITS1, 5.8S et ITS2) sitis 181 (A), 489 (T) et loco vulgo ''translation elongation factor 1-alpha'' dicto sitis 230 (G), 240 (C) et 249 (C).

No ascostromata were observed on *Eucalyptus* bark collected in the field or on inoculated *S. cordatum* or *E. grandis* branch tissue. Both on *S. cordatum* and *E. grandis* the conidiomata on inoculated branch tissue were eustromatic, superficial to slightly immersed, pulvinate without necks, sometimes conical, orange to umber when young, fuscous-black when mature (FIG. 8A, H). Stromatic tissue of base prosenchymatous (FIG. 8C). However the conidiomatal base on *S. cordatum* 90–720 µm (av. 280 µm) high above the level of bark and 140–750 µm (av. 430 µm) wide above the surface of the bark (FIG. 8H), on *E. grandis* 110–500 µm (av. 230 µm) high above the level of bark and 120–700 µm (av. 360 µm) wide above the surface of the bark (FIG. 8A). Conidiomatal locules multilocular, seldom unilocular, locules on *S. cordatum* 40–590 µm (av. 270 µm) diam (FIG. 8I), on *E. grandis* 35–640 µm (av. 290 µm) diam (FIG. 8B). Conidiophores hyaline, branched irregularly at the base or above into cylindrical cells, with or without separating septa, on *S. cordatum* (4.5–)10.0–15.0(–24.5) µm (av. 13.0 µm) long, on *E. grandis* (5.0–)11.0–16.0(–27.5) µm (av. 14 µm) long (FIG. 8E, F). Conidiogenous cells phialidic, cylindrical with or without attenuated apices, on *S. cordatum* 1.5–2.5(–3.0) µm (av. 2.0 µm) wide, on *E. grandis* 1.5–3.0(–3.5) µm (av. 2.0 µm) wide (FIG. 8E, F). Paraphyses or cylindrical sterile cells occur among conidiophores, on *S. cordatum* up to 82 µm long (av. 58 × 1.9 µm) (FIG. 8J), on *E. grandis* up to 91 µm long (av. 52 × 1.8 µm) (FIG. 8D). Conidia hyaline, non-septate, oblong to cylindrical, occasionally allantoid, extending through opening at stromatal surface as orange droplets, on *S. cordatum* (2.4–)3.3–3.7(–4.0) × (1.1–)1.3–1.6(–1.8) µm, (av. 3.5 × 1.5 µm), on *E. grandis* (2.5–)3.1–3.9(–4.3) × (1.1–)1.4–1.7(–1.9) µm, (av. 3.5 × 1.5 µm) (FIG. 8G).

Celoporthe guangdongensis differs from other species in the Asian clade of *Celoporthe* (*C. syzygii*, *C. eucalypti*, *C. indonesiensis*) by uniquely fixed DNA nucleotides in three nuclear loci, *BT1* positions 71 (T), 188 (T), 189 (C) and 194 (T); *BT2* positions 233 (–) and 234 (–); ITS (ITS1, 5.8S, ITS2) positions 181 (A) and 489 (T); *TEF-1*α positions 230 (G), 240 (C) and 249 (C).

Culture characteristics. On MEA *C. guangdongensis* is fluffy with uneven margins, white when young, turning greenish gray to greenish black after 10 d. Colony reverse smoke gray to greenish gray after 10 d. Optimal growth temperature 30 C, covering 90 mm plates after 7 d. No growth at 5 C and 35 C, and

colonies at 10 C reached 7 mm in 30 d (nearly no growth in 7 d). Asexual fruiting structures occasionally formed in primary isolations of the fungus.

Substrate. Bark of *Eucalyptus* sp.

Distribution. China.

Specimens examined. CHINA, GUANGDONG PROVINCE, *Eucalyptus* sp., *T.I. Burgess*, HOLOTYPE PREM 60468 (isolate CMW12750, artificial inoculation on South African *S. cordatum* and *E. grandis* branch tissue in Apr 2008, *S.F. Chen*), EX-TYPE culture CMW12750 = CBS128341.

Notes. Celoporthe guangdongensis is morphologically different from *C. dispersa* (paraphyses up to 39 μm), *C. indonesiensis* (paraphyses up to 50 μm), *C. syzygii* (paraphyses up to 52 μm) and *C. eucalypti* (paraphyses up to 68 μm) because of its longer paraphyses (up to 91 μm). This species was described based on the single isolate CMW12750 but supported by strong phylogenetic data and various morphological characteristics different than those of other *Celoporthe* spp.

Celoporthe indonesiensis S.F. Chen, Gryzenh., M.J. Wingf. & X.D. Zhou, gen. nov. FIG. 9
MycoBank MB519069

Etymology. Name refers to Indonesia, the country where the fungus first was collected.

Loculi conidiomatum multiloculares raro uniloculares. Conidiophorae (5.5–)12.0–18.0(–32.0) μm longae. Paraphyses usque ad 50 μm. Conidia (3.1–)3.5–4.2(–4.7) × (1.1–)1.2–1.5(–1.6) μm. A speciebis aliis cladi asiatici Celoporthis (*C. syzygii*, *C. guangdongensis*, *C. eucalypti*) nucleotidis unice fixis in tribus locis nuclearibus differt: β-tubulinum-2 sitis 235 (T), 236 (T) 238 (T); loco vulgo ''internal transcribed spacer rDNA'' dicto (ITS1, 5.8S et ITS2) sitis 40 (T), 82 (A), 84 (T), 85 (T), 211 (A) et loco vulgo ''translation elongation factor 1-alpha'' dicto sitis 76 (G), 215 (C).

No ascostromata were observed on the bark of *S. aromaticum* collected in the field or on inoculated *S. cordatum* and *E. grandis* branch tissue. Both on *S. cordatum* and *E. grandis*, the conidiomata on inoculated branch tissue were eustromatic, superficial to slightly immersed, pulvinate without necks, orange when young, umber to fuscous-black when mature (FIG. 9A, H). Stromatic tissue of base, prosenchymatous (FIG. 9C). However the conidiomatal base on *S. cordatum* 60–260 μm (av. 120 μm) high above the level of bark and 120–550 μm (av. 260 μm) wide above the surface of the bark (FIG. 9A), on *E. grandis* 60–250 μm (av. 100 μm) high above the level of bark and 100–470 μm (av. 190 μm) wide above the surface of the bark (FIG. 9H). Conidiomatal locules multilocular, seldom unilocular, locules on *S. cordatum* 50–610 μm (av. 310 μm) diam (FIG. 9B), on *E. grandis* 35–530 μm (av. 280 μm) diam (FIG. 9I). Conidiophores hyaline, branched irregularly at the base or above into cylindrical cells, with or without separating septa, on *S. cordatum* (6.0–)14.0–18.0(–29.0) μm (av. 16.0 μm) long (FIG. 9E, F), on *E. grandis* (5.5–)12.0–17.5(–32.0) μm (av. 15.0 μm) long. Conidiogenous cells phialidic, cylindrical with or without attenuated apices, on *S. cordatum* 1.5–2.5(–3.5) μm (av. 2.0 μm) wide (FIG. 9E, F), on *E. grandis* 1.0–3.0 μm (av. 2.5 μm) wide. Paraphyses or cylindrical sterile cells occur among conidiophores, on *S. cordatum* up to 48 μm long (av. 26 × 1.5 μm) (FIG. 9D), on *E. grandis* up to 50 μm long (av. 28 × 1.5 μm). Conidia hyaline, non-septate, cylindrical, occasionally oblong or allantoid, extending through opening at stromatal surface as orange droplets, on *S. cordatum* (3.1–)3.5–4.0(–4.6) × (1.1–)1.2–1.4(–1.5) μm, (av. 3.8 × 1.3 μm) (FIG. 9G), on *E. grandis* (3.5–)3.7–4.2(–4.7) × (1.1–)1.2–1.5(–1.6) μm, (av. 3.9 × 1.4 μm) (FIG. 9J).

Celoporthe indonesiensis differs from other species in the Asian clade of *Celoporthe* (*C. syzygii*, *C. eucalypti*, *C. guangdongensis*) by uniquely fixed DNA nucleotides in three nuclear loci, *BT2* positions 235 (T), 236 (T), and 238 (T); ITS (ITS1, 5.8S, ITS2) positions 40 (T), 82 (A), 84 (T), 85 (A) and 211 (A); *TEF-1α* positions 76 (G) and 215 (C).

Culture characteristics. On MEA *C. indonesiensis* fluffy with an uneven margin, white when young, turning sulfur yellow to pale luteous after 10 d. Colony reverse yellow-white to sulfur yellow after 10 d. Optimal growth temperature 30 C, covering the 90 mm plates after 6 d. No growth at 5 C and 35 C, and colonies at 10 C reached 1.5 mm in 30 d (nearly no growth in 7 d). Asexual fruiting structures occasionally form in primary isolations of the fungus.

Substrate. Bark of *Syzygium aromaticum.*

Distribution. Indonesia.

Specimens examined. INDONESIA, NORTH SUMATRA, *S. aromaticum*, Sep 1997, *M.J. Wingfield*, HOLOTYPE PREM 60469 (isolate CMW10781, artificial inoculation on South African *S. cordatum* and *E. grandis* branch tissue in Apr 2008, *S.F. Chen*), EX-TYPE culture CMW10781 = CBS115844.

Notes. Celoporthe indonesiensis is morphologically different from *C. syzygii* (conidia 2.3–3.8 μm; paraphyses up to 52 μm), *C. eucalypti* (conidia 2.6–4.4 μm; paraphyses up to 68 μm) and *C. guangdongensis* (conidia 2.4–4.3 μm; paraphyses up to 91 μm) because of its longer conidia (3.1–4.7 μm) and shorter paraphyses (up to 50 μm). Furthermore its conidia are shorter and paraphyses are longer than those of *C. dispersa* (conidia 2.5–5.5 μm; paraphyses up to 39 μm). At 10 C on 2% MEA after 30 d *C. indonesiensis* grew slower (av. colony diam = 1.5 mm) than *C. guangdongensis* (av. colony diam = 7 mm), *C. eucalypti* (av. colony diam = 16 mm), and *C. syzygii* (av. colony

diam = 31.5 mm). This species is described based on the phylogenetic placement of three isolates (CMW10779, CMW10780, CMW10781), the morphology of a single isolate (CMW10781) and is supported by strong phylogenetic and morphological differences from other *Celoporthe* spp.

DICHOTOMOUS KEY TO *CELOPORTHE* SPECIES

The key is based on characteristics of naturally occurring and artificially induced conidia and paraphyses, as well as growth in culture:

1a. Optimal growth at 25 C; conidia longer than 5 µm; paraphyses shorter than 40 µm; conidiomata unilocular, occasionally multilocular; Asci* shorter than 35 µm . . . . . *C. dispersa*
1b. Optimal growth at 30 C; conidia shorter than 5 µm; paraphyses longer than 45 µm; conidiomata multilocular, occasionally unilocular; Asci* longer than 40 µm 2
2a. Conidia longer than 4.5 µm, cylindrical, occasionally oblong . . . . . *C. indonesiensis*
2b. Conidia shorter than 4.5 µm, oblong, occasionally allantoid 3
3a. Conidia shorter than 4 µm . . . . . *C. syzygii*
3b. Conidia longer than 4 µm 4
4a. Paraphyses shorter than 70 µm . . . . . *C. eucalypti*
4b. Paraphyses longer than 90 µm . . . *C. guangdongensis*

* Teleomorph structures have not been seen for *C. eucalypti*, *C. guangdongensis* or *C. indonesiensis*.

SYNOPTIC KEY TO *CELOPORTHE* SPECIES

Optimum growth:
- a. 25 C: *C. dispersa*
- b. 30 C: *C. eucalypti*, *C. guangdongensis*, *C. indonesiensis*, *C. syzygii*

Ascus size:*
- a. Asci shorter than 35 µm: *C. dispersa*
- b. Asci longer than 40 µm: *C. syzygii*

Conidiomatal locules:
- a. Unilocular, occasionally multilocular: *C. dispersa*
- b. Multilocular, occasionally unilocular: *C. eucalypti*, *C. guangdongensis*, *C. indonesiensis*, *C. syzygii*

Conidia morphology (length):
- a. Up to 4 µm: *C. syzygii*
- b. Up to 4.5 µm: *C. eucalypti*, *C. guangdongensis*
- c. Up to 4.75 µm: *C. indonesiensis*
- d. Up to 5.5 µm: *C. dispersa*

Paraphyses morphology (length):
- a. Up to 40 µm: *C. dispersa*
- b. Up to 50 µm: *C. indonesiensis*
- c. Slightly longer than 50 µm: *C. syzygii*
- d. Up to 70 µm: *C. eucalypti*
- e. Up to 90 µm: *C. guangdongensis*

Conidial morphology:
- a. Conidia mostly cylindrical, occasionally oblong or allantoid: *C. indonesiensis*
- b. Conidia mostly oblong, occasionally allantoid: *C. dispersa*, *C. eucalypti*, *C. guangdongensis*, *C. syzygii*

* Teleomorph structures have not been seen for *C. eucalypti*, *C. guangdongensis* or *C. indonesiensis*.

Pathogenicity tests.—Glasshouse trials. The three isolates of *C. eucalypti* (CMW26900, CMW26908, CMW26911) tested for pathogenicity on *Eucalyptus* clone TAG-5 in the glasshouse produced lesions within 6 wk, while wounds were covered with callus tissue in the case of the control inoculations (FIG. 11). Mean comparison tests showed that the lesion lengths produced by the *C. eucalypti* isolates were significantly longer ($P < 0.0001$ to $P = 0.0047$) than those of the controls (FIG. 11). Analyses of variance showed significant differences in susceptibility of the *Eucalyptus* clone to the fungal isolates ($P = 0.0433$). Of the isolates tested lesions produced by isolate CMW26908 were the longest, differing significantly from isolate CMW26900 and the controls (FIG. 11). All the inoculated fungi were successfully re-isolated from the lesions, while *Celoporthe* was not isolated from the control inoculations. Based on the glasshouse trial, the most virulent isolate, CMW26908, was chosen for use in field inoculations.

Field trials. Statistically significant differences in lesion lengths on the seven *Eucalyptus* genotypes were found between the isolates identified as *C. eucalypti* (CMW26908) and *C. guangdongensis* (CMW12750), and the control inoculations ($P < 0.0001$ to $P = 0.0230$) after 5 wk under field conditions (FIG. 12). *Eucalyptus* genotypes CEPT-2 and CEPT-6 were the most susceptible to both *Celoporthe* spp., while genotypes CEPT-3, CEPT-4 and CEPT-5 were relatively

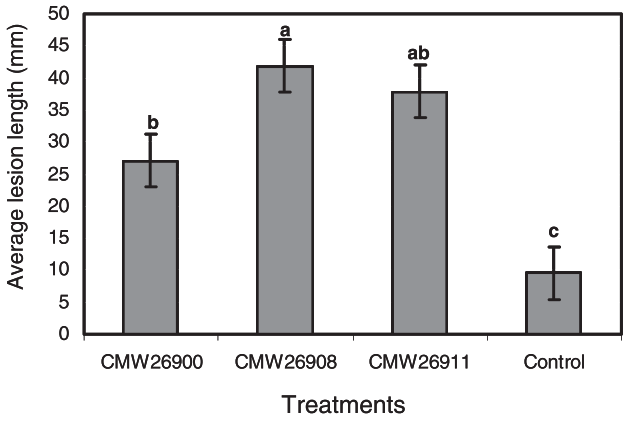

FIG. 11. Histogram showing the average lesion lengths (mm) resulting from inoculations onto *E. grandis* clone (TAG-5) under glasshouse conditions. Three isolates of *C. eucalypti* from *Eucalyptus* trees in China were used. Bars represent 95% confidence limits for each treatment. Letters above the bars indicate treatments that statistically were significantly different ($P = 0.05$).

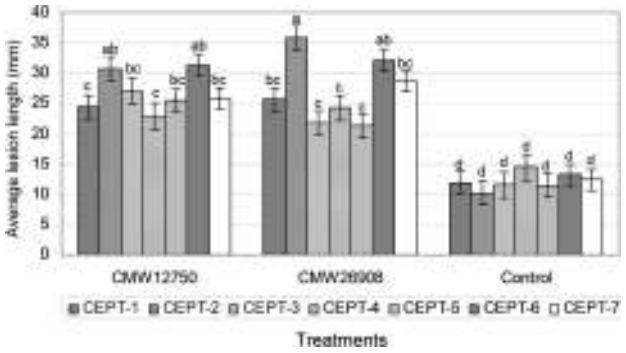

FIG. 12. Histogram showing the average lesion lengths (mm) resulting from inoculations of seven *Eucalyptus* genotypes with isolate CMW12750 (*C. guangdongensis*) and isolate CMW26908 (*C. eucalypti*). Bars represent 95% confidence limits for each treatment. Different letters above the bars indicate treatments that statistically were significantly different ($P = 0.05$).

tolerant to infection by *C. eucalypti* and *C. guangdongensis* (FIG. 12).

The trial, including three *C. syzygii* isolates (CMW24912, CMW24914, CMW24917), *C. eucalypti* (CMW26908) and *C. guangdongensis* (CMW12750) on two *Eucalyptus* genotypes (CEPT-6, CEPT-7), showed that the *Celoporthe* isolates produced significantly longer lesions ($P < 0.0001$ to $P = 0.0380$) on the two tested *Eucalyptus* genotypes than the control inoculations that had started to heal through the production of callus tissue (FIG. 13A). Analyses of variance showed significant differences ($P < 0.001$) in susceptibility between the two *Eucalyptus* genotypes, with CEPT-6 being more susceptible to infection by *C. guangdongensis* (CMW12750) and *C. syzygii* (CMW24912, CMW24914, CMW24917) than CEPT-7 ($P < 0.0001$ to $P = 0.0302$) (FIG. 13A). No statistically significant differences were found between CEPT-6 and CEPT-7 for *C. eucalypti* (CMW26908) ($P = 0.1621$). No differences were found between the *C. syzygii* isolates and the two *Celoporthe* spp. that originated from *Eucalypts* on clone CEPT-6 ($P = 0.0676$ to $P = 1.0000$), however on CEPT-7 the *Eucalyptus* isolates CMW26908 (*C. eucalypti*) and CMW12750 (*C. guangdongensis* showed higher virulence on *Eucalypts* than the *C. syzygii* isolates.

The three *Celoporthe* spp. inoculated onto the branches of *S. cumini* produced significantly ($P < 0.0001$) longer lesions than the control inoculations after 6 wk (FIG. 13B). The analyses showed no statistical differences between the two sets of inoculations ($P = 0.2421$) and therefore the data were combined. Analyses of variance for the combined data showed significant differences in susceptibility to the fungal isolates ($P = 0.0004$). For example the *C.*

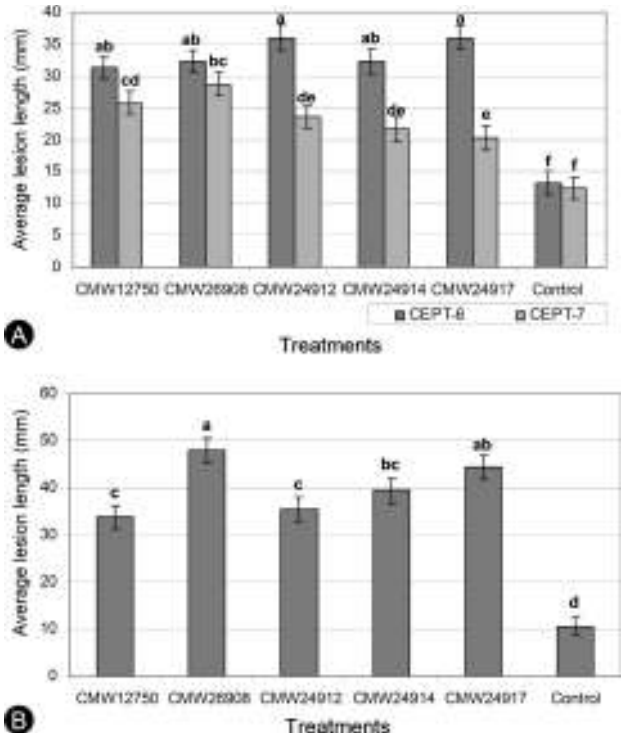

FIG. 13. Histogram showing average lesion lengths (mm) resulting from inoculation of (A). Two *Eucalyptus* genotypes (CEPT-6, CEPT-7) and (B). *S. cumini* branches with three isolates (CMW24912, CMW24914, CMW24917) of *C. syzygii*, one isolate (CMW26908) of *C. eucalypti* and one isolate (CMW12750) of *C. guangdongensis*. Bars represent 95% confidence limits for each treatment. Letters above the bars indicate treatments that statistically were significantly different ($P = 0.05$).

eucalypti isolate (CMW26908) produced significantly ($P = 0.0001$ to $P = 0.0215$) longer lesions than the *C. guangdongensis* isolate (CMW12750) and the *C. syzygii* isolates (CMW24912, CMW24914; FIG. 13B).

DISCUSSION

In this study four previously undescribed species of *Celoporthe* were found on bark collected from diseased *Syzygium* and *Eucalyptus* trees in Asia. *C. syzygii* was collected from *S. cumini* trees in China, both *C. eucalypti* and *C. guangdongensis* from non-native *Eucalyptus* trees in China and *C. indonesiensis* isolates originated from *S. aromaticum* trees in Indonesia. The identification of these species was supported by phylogenetic analyses and SNP determination as well as morphological characteristics. The species from *Eucalyptus* in China also were shown to be capable of causing lesions on commercially utilized *Eucalyptus* genotypes and on branches of *S. cumini* trees.

In this study anamorph fruiting structures were successfully induced on *Eucalyptus* and *Syzygium*

branch sections for all of the *Celoporthe* isolates. Differences were observed between the naturally occurring anamorph structures for *C. syzygii* and those formed on the inoculated branch sections, especially relating to the shape and position of conidiomata. However characteristics, such as diameter of conidiomata, sizes of conidiophores, conidigenous cells and conidia in *C. syzygii*, were similar in the artificially induced and naturally occurring fruiting structures and they therefore were useful in distinguishing between the four Asian phylogenetic *Celoporthe* spp.

Phylogenetic analyses for isolates of *Celoporthe* suggested clustering of species based on geographic origin and host. Thus the three Chinese *Celoporthe* spp. were more closely related to each other than to Indonesian *C. indonesiensis*. In contrast the Chinese *C. eucalypti* and *C. guangdongensis* from *Eucalyptus* in China were more closely related to each other than to *C. syzygii* from *Syzygium*. Similarly the *Celoporthe* species formed two major clades, one including *C. dispersa* from Africa and the other including the Asian species described in the present study. Nakabonge et al. (2006a) also suggested clustering of *Celoporthe* isolates from South Africa, based on host and regions of collection, but they were not able to explain these results due to the limited number of isolates available.

The discovery of the *Celoporthe* spp. in Asia raises interesting questions regarding the origin of these fungi. Nakabonge et al. (2006a) suggested that *C. dispersa* might have originated from native African Myrtales. Similarly all four *Celoporthe* spp. that were identified from non-native trees in this study might have originated from native Myrtales in southern or southeastern Asia. This is especially likely due to the species diversity of *Celoporthe* in Asia. Additional surveys however are necessary to expand the host and geographic ranges of *Celoporthe* spp. in southeastern Asia and other regions to obtain a better indication of their possible origins.

Research showed that some pathogens in the Cryphonectriaceae may undergo host shifts (Slippers et al. 2005), enabling them to infect tree species other than their native hosts (Wingfield 2003; Gryzenhout et al. 2004, 2006b, 2009, 2010; Heath et al. 2006; Nakabonge et al. 2006a, b; Begoude et al. 2010; Vermeulen et al. 2011). It has been suggested further that species of *Chrysoporthe* that infect non-native plantation-grown *Eucalyptus* have originated from native trees in the Myrtales (Gryzenhout et al. 2004; Rodas et al. 2005; Heath et al. 2006; Gryzenhout et al. 2006b, 2009, 2010). A similar host shift could have occurred with *C. dispersa* and the four *Celoporthe* spp. described in this study. In the present study all four *Celoporthe* spp. were isolated from non-native trees in Asia. This includes *C. indonesiensis*, which was found on planted *S. aromaticum* trees in northern Sumatra, Indonesia, where these trees do not occur naturally. The ability of the four *Celoporthe* spp. to infect *Syzygium* trees that are native to southern and southeastern Asia suggests that these fungi could have originated from these or related trees and that they have undergone host shifts to infect *Eucalyptus* species.

The pathogenicity tests in this study showed that Chinese *Celoporthe* spp. from *S. cumini* and *Eucalyptus* are pathogenic to various *Eucalyptus* genotypes and *S. cumini* trees. Similar lesion sizes also were produced on both *Eucalyptus* genotypes and *S. cumini* trees by *Chr. deuterocubensis* (Chen et al. 2010), which suggests that *Celoporthe* spp. might be equally important potential pathogens of *Eucalyptus* in China. Similar to the results of the screening trials with *Chr. deuterocubensis* in China (Chen et al. 2010), the inoculations in this study showed that *Eucalyptus* genotypes differ in susceptibility to infection by *Celoporthe* spp. These results further imply that it will be possible to select *Eucalyptus* planting stock with tolerance to infection by these fungi.

Pathogenicity tests showed that cross infectivity between *Eucalyptus* and *Syzygium* is possible by the *Celoporthe* spp. described in thus study. For example the isolates of *C. syzygii* collected from *Syzygium* trees were more pathogenetic on the tested *Eucalyptus* genotype CEPT-6 than isolates of *C. eucalypti* and *C. guangdongensis* from *Eucalyptus* trees. Likewise the isolate of *C. eucalypti* collected from an *Eucalyptus* clone was more pathogenic on *Syzygium* trees than the isolates of *C. syzygii* collected from *Syzygium*. Pathogenicity studies with *C. dispersa* have shown that an isolate of this fungus collected from *Tibouchina granulosa* Cogn.: Britton was more pathogenic on an *Eucalyptus* clone than on *T. granulosa* plants (Nakabonge et al. 2006a). The cross infectivity of *Celoporthe* spp. on different hosts suggests that quarantine regulations should consider these alternative hosts to prevent the pathogens from moving to new areas.

ACKNOWLEDGMENTS

This study was initiated through the bilateral agreement between South Africa and China, and financially supported through projects 2007DFA31190, 2008B050100014 and 10145624536-400000. We also appreciate the financial and logistical support of the members of Tree Protection Co-operative Programme (TPCP) and Dr Treena I. Burgess (Murdoch University, Australia) for providing some isolates used in this study. We are grateful for the help of Prof Hennie Groeneveld and Dr Mike van der Linde who assisted with the statistical analyses, Dr Hugh Glen who provided the Latin description, Miss Marcele Vermeulen

for the *TEF-1α* sequence data for *Celoporthe dispersa*, and colleagues of LeiZhou Forestry Bureau, XinTao Mou, GuiXiang Zhao and ChunYan Xie for their valuable assistance in the field.

LITERATURE CITED

Anagnostakis SL. 1987. Chestnut blight: the classical problem of an introduced pathogen. Mycologia 79: 23–37, doi:10.2307/3807741

———. 1992. Chestnuts and the introduction of chestnut blight. Ann Rep N Nut Grow Assoc 83:39–42.

Begoude BAD, Gryzenhout M, Wingfield MJ, Roux J. 2010. *Aurifilum*, a new fungal genus in the Cryphonectriaceae from *Terminalia* species in Cameroon. Anton Leeuw Int J G 98:263–278, doi:10.1007/s10482-010-9467-8

Carbone I, Kohn LM. 1999. A method for designing primer sets for speciation studies in filamentous ascomycetes. Mycologia 91:553–556, doi:10.2307/3761358

Castlebury LA, Rossman AY, Jaklitsch WJ, Vasilyeva LN. 2002. A preliminary overview of the Diaporthales based on large subunit nuclear ribosomal DNA sequences. Mycologia 94:1017–1031, doi:10.2307/3761867

Cheewangkoon R, Groenewald JZ, Summerell BA, Hyde KD, To-anun C, Crous PW. 2009. Myrtaceae, a cache of fungal biodiversity. Persoonia 23:55–85.

Chen SF, Gryzenhout M, Roux J, Xie YJ, Wingfield MJ, Zhou XD. 2010. Identification and pathogenicity of *Chrysoporthe cubensis* on *Eucalyptus* and *Syzygium* species in south China. Plant Dis 94:1143–1150, doi:10.1094/PDIS-94-9-1143

Fairchild D. 1913. The discovery of the chestnut bark disease in China. Science 38:297–299, doi:10.1126/science.38.974.297

Farris JS, Kallersjo M, Kluge AG, Bult C. 1995. Testing significance of incongruence. Cladistics 10:315–319, doi:10.1111/j.1096-0031.1994.tb00181.x

Felsenstein J. 1985. Confidence intervals on phylogenetics: an approach using bootstrap. Evolution 39:783–791, doi:10.2307/2408678

Glass NL, Donaldson GC. 1995. Development of primersets designed for use with the PCR to amplify conserved genes from filamentous ascomycetes. Appl Environ Microbiol 61:1323–1330.

Gryzenhout M, Myburg H, van der Merwe NA, Wingfield BD, Wingfield MJ. 2004. *Chrysoporthe*, a new genus to accommodate *Cryphonectria cubensis*. Stud Mycol 50: 119–142.

———, ———, Wingfield BD, Wingfield MJ. 2006a. *Cryphonectriaceae* (Diaporthales), a new family including *Cryphonectria*, *Chrysoporthe*, *Endothia* and allied genera. Mycologia 98:239–249, doi:10.3852/mycologia.98.2.239

———, Rodas CA, Menas Portales J, Clegg P, Wingfield BD, Wingfield MJ. 2006b. Novel hosts of the *Eucalyptus* canker pathogen *Chrysoporthe cubensis* and a new *Chrysoporthe* species from Colombia. Mycol Res 110: 833–845, doi:10.1016/j.mycres.2006.02.010

———, Tarigan M, Clegg PA, Wingfield MJ. 2010. *Cryptometrion aestuescens* gen. sp. nov. (*Cryphonectriaceae*) pathogenic to *Eucalyptus* in Indonesia. Australas Plant Path 39:161–169, doi:10.1071/AP09077

———, Wingfield BD, Wingfield MJ. 2009. Taxonomy, phylogeny and ecology of bark-inhabiting and tree pathogenic fungi in the Cryphonectriaceae. St Paul, Minnesota: APS Press. 119 p.

Guindon S, Gascuel O. 2003. A simple, fast and accurate algorithm to estimate large phylogenies by maximum likelihood. Syst Biol 52:696–704, doi:10.1080/10635150390235520

Heath R, Gryzenhout M, Roux J, Wingfield MJ. 2006. Discovery of the canker pathogen *Chrysoporthe austroafricana* on native *Syzygium* spp. in South Africa. Plant Dis 90:433–438, doi:10.1094/PD-90-0433

Hillis DM, Huelsenbeck JP. 1992. Signal, noise and reliability in molecular phylogenetic analyses. J Hered 83:189–195.

Hodges CS, Alfenas AC, Ferreira FA. 1986. The conspecificity of *Cryphonectria cubensis* and *Endothia eugeniae*. Mycologia 78:343–350, doi:10.2307/3793037

Huelsenbeck JP, Bull JJ, Cunningham CW. 1996. Combining data in phylogenetic analysis. Trends Ecol Evol 11: 152–158, doi:10.1016/0169-5347(96)10006-9

Katoh K, Misawa K, Kuma K, Miyata T. 2002. MAFFT: a novel method for rapid multiple sequence alignment based on fast Fourier transform. Nucleic Acids Res 30: 3059–3066, doi:10.1093/nar/gkf436

Kobayashi T, Itô K. 1956. Two new species of *Endothia*. Ann Phytopathol Soc Japan 21:151–152.

Myburg H, Gryzenhout M, Wingfield BD, Milgroom MG, Shigeru K, Wingfield MJ. 2004. DNA sequence data and morphology define *Cryphonectria* species in Europe, China and Japan. Can J Bot 82:1730–1743, doi:10.1139/b04-135

———, ———, ———, Wingfield MJ. 2002. β-tubulin and Histone *H3* gene sequences distinguish *Cryphonectria cubensis* from South Africa, Asia and South America. Can J Bot 80:590–596, doi:10.1139/b02-039

———, ———, ———, ———. 2003. Conspecificity of *Endothia eugeniae* and *Cryphonectria cubensis*: a re-evaluation based on morphology and DNA sequence data. Mycoscience 44:187–196.

———, Wingfield BD, Wingfield MJ. 1999. Phylogeny of *Cryphonectria cubensis* and allied species inferred from DNA analysis. Mycologia 91:243–250, doi:10.2307/3761369

Nakabonge G, Gryzenhout M, Roux J, Wingfield BD, Wingfield MJ. 2006a. *Celoporthe dispersa* gen. et sp. nov. from native *Myrtales* in South Africa. Stud Mycol 55:255–267, doi:10.3114/sim.55.1.255

———, Roux J, Gryzenhout M, Wingfield MJ. 2006b. Distribution of *Chrysoporthe* canker pathogens on *Eucalyptus* and *Syzygium* species in eastern and southern Africa. Plant Dis 90:734–740, doi:10.1094/PD-90-0734

Nylander JAA. 2004. MrModeltest 2.3. Program distributed by the author. Uppsala, Sweden: Evolutionary Biology Centre, Uppsala Univ.

Posada D, Crandall KA. 1998. Modeltest: testing the model of DNA substitution. Bioinformatics 14:817–818, doi:10.1093/bioinformatics/14.9.817

Rayner RW. 1970. A mycological colour chart. Kew, Surrey, UK: Commonwealth Mycological Institute and British Mycological Society. 34 p.

Rehner SA, Samuels GJ. 1994. Taxonomy and phylogeny of *Gliocladium* analysed from nuclear large subunit ribosomal DNA sequences. Mycol Res 98:625–634, doi:10.1016/S0953-7562(09)80409-7

Rodas CA, Gryzenhout M, Myburg H, Wingfield BD, Wingfield MJ. 2005. Discovery of the *Eucalyptus* canker pathogen *Chrysoporthe cubensis* on native *Miconia* (*Melastomataceae*) in Colombia. Plant Path 54:460–470, doi:10.1111/j.1365-3059.2005.01223.x

Ronquist F, Huelsenbeck JP. 2003. MrBayes 3: Bayesian phylogenetic inference under mixed models. Bioinformatics 19:1572–1574, doi:10.1093/bioinformatics/btg180

SAS Institute Inc. 1999. SAS/STAT 8 users' guide. Cary, North Carolina: SAS Institute Inc.

Sharma JK, Mohanan C, Florence EJM. 1985. Occurrence of *Cryphonectria* canker disease of *Eucalyptus* in Kerala, India. Ann Appl Biol 106:265–276, doi:10.1111/j.1744-7348.1985.tb03116.x

Shear CL, Stevens NE. 1913. The chestnut blight parasite (*Endothia parasitica*) from China. Science 38:295–297, doi:10.1126/science.38.974.295

———, ———. 1916. The discovery of the chestnut blight parasite (*Endothia parasitica*) and other chestnut fungi in Japan. Science 43:173–176, doi:10.1126/science.43.1101.173-a

Slippers B, Crous PW, Denman S, Coutinho TA, Wingfield BD, Wingfield MJ. 2004. Combined multiple gene genealogies and phenotypic characters differentiate several species previously identified as *Botryosphaeria dothidea*. Mycologia 96:83–101, doi:10.2307/3761991

———, Stenlid J, Wingfield MJ. 2005. Emerging pathogens: Fungal host jumps following anthropogenic introduction. Trends Ecol Evol 20:420–421, doi:10.1016/j.tree.2005.05.002

Swofford DL. 2002. PAUP* 4.0: phylogenetic analysis using parsimony (*and other methods). Sunderland, Massachusetts: Sinauer Associates.

Tamura K, Dudley J, Nei M, Kumar S. 2007. MEGA4: molecular evolutionary genetics analysis (MEGA) software. Mol Biol Evol 24:1596–1599, doi:10.1093/molbev/msm092

Teng SC. 1934. Notes on Sphaeriales from China. Sinensia 4:359–433.

van der Merwe NA, Gryzenhout M, Steenkamp ET, Wingfield BD, Wingfield MJ. 2010. Multigene phylogenetic and population differentiation data confirm the existence of a cryptic species within *Chrysoporthe cubensis*. Fungal Biol 114:966–979, doi:10.1016/j.funbio.2010.09.007

Vermeulen M, Gryzenhout M, Wingfield MJ, Roux J. 2011. New records of Cryphonectriaceae from southern Africa including *Latruncellus aurorae* gen. sp. nov. Mycologia 103:554–569, doi:10.3852/10-283

Vilgalys R, Hester M. 1990. Rapid genetic identification and mapping of enzymatically amplified ribosomal DNA from several *Cryptococcus* species. J Bacteriol 172:4238–4246.

White TJ, Bruns T, Lee S, Taylor J. 1990. Amplification and direct sequencing of fungal ribosomal RNA genes for phylogenetics. In: Innis AM, Gelfand DH, Sninsky JJ, White TJ, eds. PCR protocols: a guide to methods and applications. San Diego: Academic Press. p 315–322.

Wingfield MJ. 2003. Increasing threat of diseases to exotic plantation forests in the southern hemisphere: lessons from Cryphonectria canker. Australas Plant Path 32:133–139, doi:10.1071/AP03024

Zhang N, Blackwell M. 2001. Molecular phylogeny of dogwood anthracnose fungus (*Discula destructiva*) and the Diaporthales. Mycologia 93:355–365, doi:10.2307/3761657

Zhou X, Xie Y, Chen SF, Wingfield MJ. 2008. Diseases of eucalypt plantations in China: challenges and opportunities. Fungal Divers 32:1–7.